PREDICTION OF PERMEABILITY IN COMPRESSED POLYURETHANE FOAMS IN VACUUM ASSISTED INFILTRATION PROCESS

By

BALAJI RAMANUJAKANNAN

Bachelor of Science in Mechanical Engineering
ANNA UNIVERSITY
Chennai, Tamilnadu, India
2005

Submitted to the Faculty of the
Graduate College of
Oklahoma State University
in partial fulfillment of
the requirements for
the Degree of
MASTER OF SCIENCE
May, 2011

PREDICTION OF PERMEABILITY IN COMPRESSED POLYURETHANE FOAMS IN VACUUM ASSISTED INFILTRATION PROCESS

Thesis Approved:

Dr. Raman P. Singh

Thesis Advisor

Dr. Ranji Vaidyanathan

Dr. Khaled A. Sallam

Dr. A. Gordon Emslie

Dean of the Graduate College

ACKNOWLEDGMENTS

Pursuing my master's degree here at Oklahoma State University had been an experience of sorts. I would say it was like participating in a supercross championship with frequent steering jumps that I could relate to some daunting task in research. Passing every steering jump was critical, as it gave the needed leap in every bottleneck of research. Though it wasn't a cakewalk, this race was made less daunting and more enjoyable from the continuous support and tutelage of my research advisor, Dr. Raman P. Singh. Thankyou, is honestly a small word for acknowledging all his support throughout my association with MAML. As they say in boxing, Always finish stronger than you start, is probably one of the important lessons that I have learnt from him.

I would like to thank Dr. Ranji Vaidyanathan and Dr. Khalled Sallam for being in my thesis committee. Discussions with them were much beneficial and brainstorming.

I extend my sincere gratitude to Mr.Ron Workman of ETS-Lingren. He was very quick in his response for whatever that I needed in my work. Also, I would thank the Oklahoma Centre for Advanced Science and Technology (OCAST) for funding this project.

I am thankful to Dr. Gajendra Pandey for all the valuable guidance he provided on various aspects of my work. I am also thankful to Fu Boshen, Graduate student at OSU's web handling research center for his expertise suggestions in ABAQUS.

A great deal of help was offered from time to time by one of my very good pal and room

mate, Vasudevan a.k.a Silent Killer. Chaitanya (Chattie), was blissful and was a patient room mate. Life at MAML was more fun with these guys

I should express my deepest gratitude for Leila and Masood. They were one such beautiful couples and never said no for any help that we needed. Masood's insight on any topic of his interest and Leila's kindness needs a special mention. Also, I'm thankful to Ms.Seshumani Vorrey and Dr.Pranav Nawani.

I was fortunate to have great friends/ lab-mates at MAML. Arif Rahman is technically smart and down to earth. Sadia and Hamim were all ears to my self proclaimed funny jokes. Suman shared a similar physique as mine and is strong in his technical domain. Phil Rogers was probably one of the coolest guys around and Abhishek Jain was popular for his flair towards tamil (my mother tongue) songs. I am also thankful to Kunal Mishra (Rajinikanth from Delhi), Austin Beerwinkle, Mohammed Husien and Abhisek Bhadra. I would like to extend a special acknowledgement to Dhivakar for his help in proofreading my document. Chirag was a dynamite and it was so much fun hanging out with him every-time.

I would also like to thank all my friends both at Stillwater and Tulsa, for all the affection they showered, which made me less prone to home sickness.

My other room mates Rengarajan and Krishna were so patient and never let me stay in hunger. Though trivial, I should thank the manufacturers of Top ramen noodles and Walmart's orange-pinenapple cookies. They were life saviors.

Finally, I would like to thank my mom, dad and my sister, for their unwilling love and support without whom I would not have reached this stage!!!

TABLE OF CONTENTS

LIST OF TABLES

Table Page

LIST OF FIGURES

CHAPTER 1

INTRODUCTION

1.1 Problem Statement

Globally, largest category of cellular polymeric materials are constituted by polyurethane foams, and they are used in versatile applications [3]. By its very nature of elastic cell structures, the performances that are gained will be in the form of multi-levels and can be matched to different end uses. In todays home furnishing industry, among all the cushioning materials available, flexible polyurethane foams have the greatest advantage — the ability to be predicted fairly upon the given performance requirements that are extremely sensitive to applications. These foams are used in domestic furniture as cushioning materials, and in refrigerators as thermal insulating panels [4]. Other specific applications include, anechoic/acoustic chambers and radio-frequency shielding/absorbing blocks.

ETS-Lindgren, a company based in Durant, Oklahoma, manufactures numerous products based on polyurethane foams for many such applications. The precursor raw material is treated using carbon black loading and fire retardant salts. However, the current nature of the fabrication process that is followed at the ETS-Lindgren and most of its competitors results in generation of significant quantity of scrap polyurethane foam loaded with toxic chemicals. The biggest drawback is that, these foams have to chemically treated to remove hazards before being disposed to landfills. This leads to very high-cost material, that, if utilized, would lead to significant benefits. An alternative technique was initially proposed to eliminate the carbon-black loaded scraps by introducing a novel vacuum assisted infiltration (VAI) process. Using this technique, carbon-black is directly infiltrated

onto the required foam block shapes with negligible amount of waste. For better dispersion of the infiltrated liquid across the compressed polyurethane foam sample, one must accurately analyze foam compression to predict its permeability at different strain rates. Hence, this study has been primarily aimed at predicting the permeability of a compressed polyurethane foam block in the VAI process.

1.2 Foam Structure and Its Types

Foams are essentially a huge network of tiny three-dimensional cellular structures that resemble a structure of a honeycomb shaped in twelve five-sided planes. Polyurethane foams can be broadly classified into two categories: open cell foam (flexible foam) and closed cell (rigid foam).

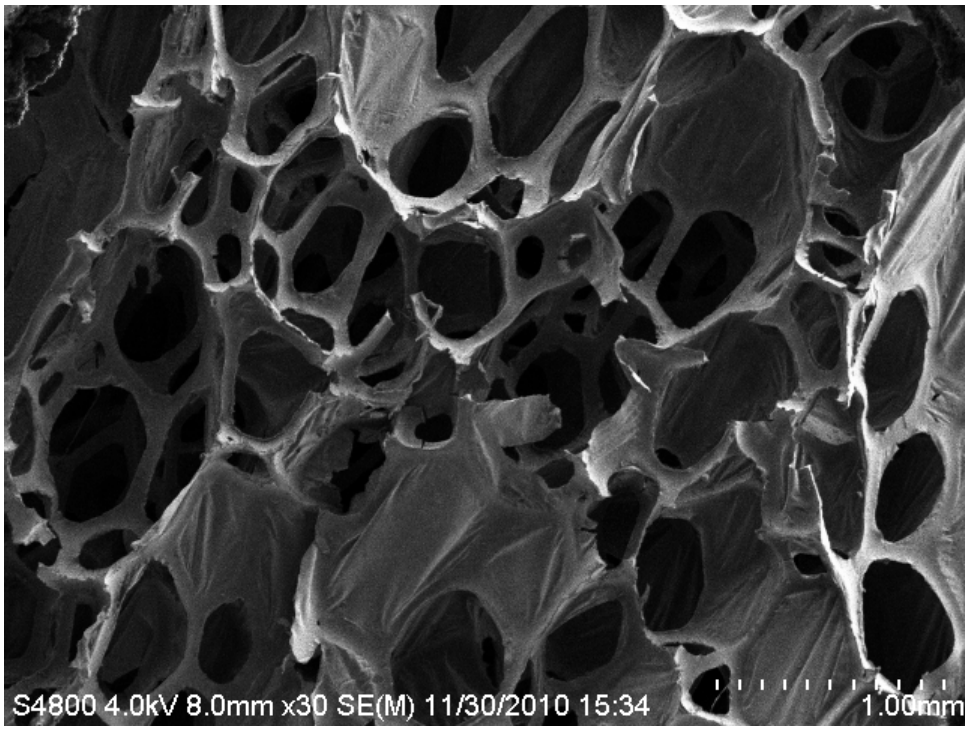

Figure 1.1: A typical microstructure of an open cell foam

Open cell foam contains pores that are interconnected through a relatively soft networks. They are mainly made up of two parts: struts/cell walls and voids/open window

areas. When a force is applied, the strut and void structure allows air to pass through the foam material. As shock absorbers perform in a car, the elastic nature of the strut walls acts as a shock absorber that allows the foam to come back to its original shape after compression.

On the other hand, closed cell foam does not have interconnected pores, but possess higher compressive strengths due to their relatively strong nature of the structure. However, these foams are generally dense, require more material, and hence more expensive to produce. Open cell foams are primarily used for cushioning purposes where comfort is mainly needed, while the closed cell foams are primarily used as thermal insulators in refrigerators, and building panels for other insulating applications. Both open and closed cell foams are widely used in sandwich composites as core materials.

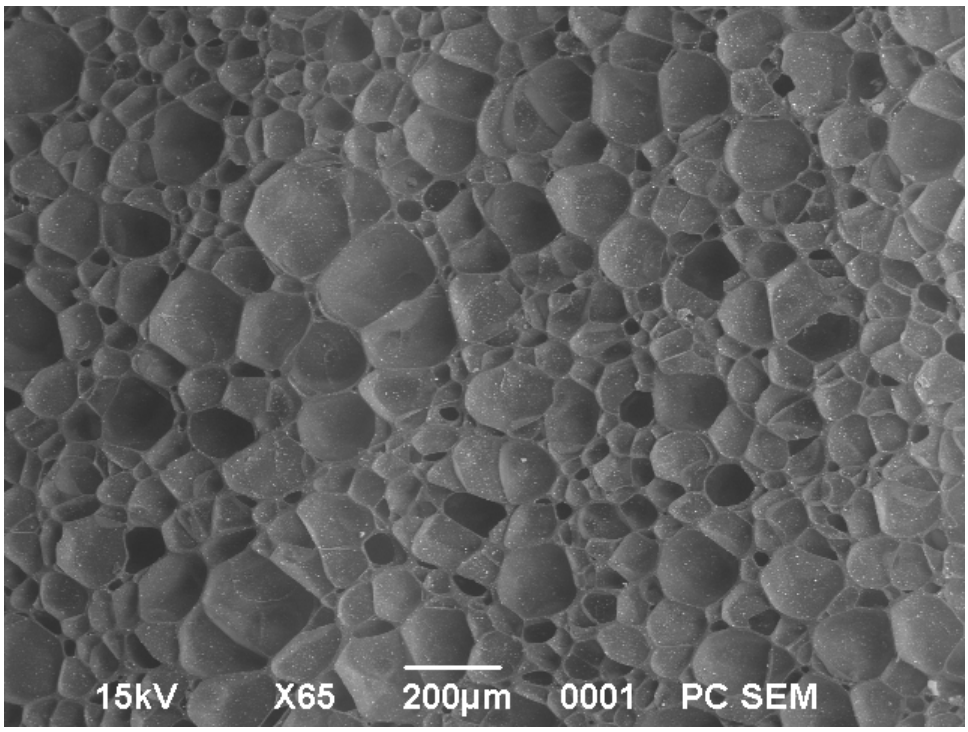

Figure 1.2: A typical microstructure of closed cell foam [1]

Open cell foams are increasingly used in acoustic mass applications for treating the high energy sounds waves that are generated from various sources. They are essentially

cut into wedge/pyramidal forms to facilitate the breaking down of the sound waves in anechoic chambers. These wedge foams attenuate airborne sound waves by exhibiting high resistance to air, and thereby reducing the wave amplitudes. Energy is finally dissipated as heat. They are treated with dyes and fire retardants to prevent them from catching fire. Pyramidal foam blocks are also used as a radio frequency absorbers whose working range is 100 MHz–40 GHz [5]. The physical size of the foam pyramid determines the lowest useable frequency. The larger the pyramid dimensions, lower the operational frequency.

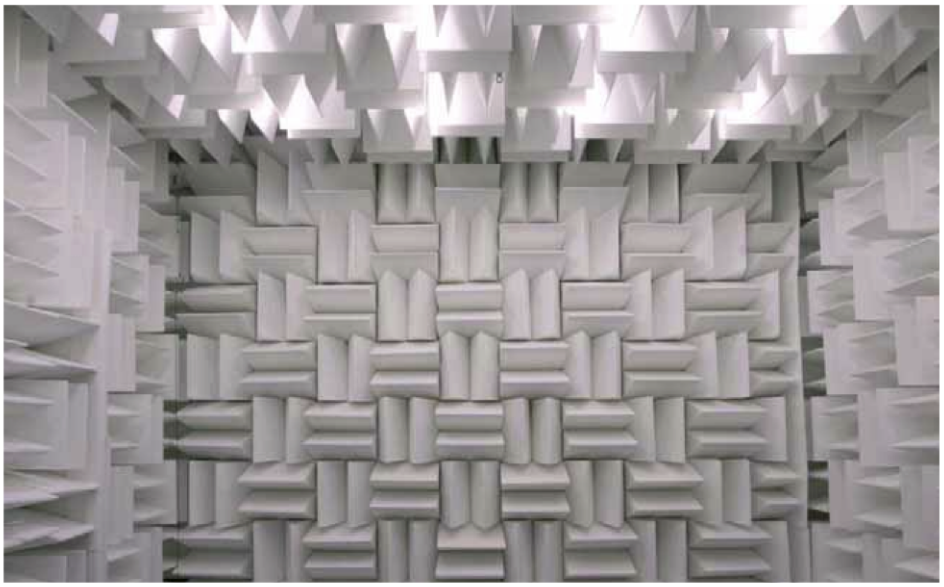

Figure 1.3: Anechoic chamber [2]

Typically, anechoic chambers have interior walls stacked with pyramidal shaped polyurethane foam blocks infused with fire retardants. They are either radiation absorbent or acoustic absorbent based and insulated from exterior noise sources. Generally in anechoic chambers, carbon-black is used in pyramidal polyurethane foams, and it acts as a lossy material for absorbing electromagnetic radiation.

1.3 Current Method Followed by ETS-Lindgren-Lindrgren

ETS-Lindgren fabricates acoustic and electrical absorber materials using a two step precess. First a solid block of open cell polyurethane foam is immersed in a bath of carbon black, to give suitable electrical characteristics, and then treated with fire retardant salts for safety. Then, the foam is cut into complex pyramidal shapes to fabricate absorber components, that are assembled into various shielding and test systems.

However, the current fabrication methodology result in significant quantity of scrap of polyurethane foam from the nature of the fabrication process. This scrap foam represents a high-value and high-cost material, as it has been treated and processed to provide electrical, acoustic, and fire retardant characteristics. Currently, this foam cannot be recycled or reused and must be discarded at a considerable cost.

The disadvantage of the current method followed at ETS-Lindgren is two fold, as it increases the cost of production due to high scrap from the processed material. It also increases the cost of disposal, because the foam contains fire retardant salts that can leach out in landfills and therefore require expensive environmental remediation. Reuse of this valuable resource would provide this organization a distinct competitive advantage compared to other manufacturers.

1.3.1 Proposed Technique and Measures

To eliminate the high-cost arising from the current fabrication method, a new technique was proposed to employ VAI process directly onto the complex pyramidal foams. In the proposed technique, the initial solid blocks of open cell polyurethane foams are cut to the required pyramidal block dimensions [6] and they are infused with carbon-black solution using vacuum assisted infiltration process for better electrical conductivity.

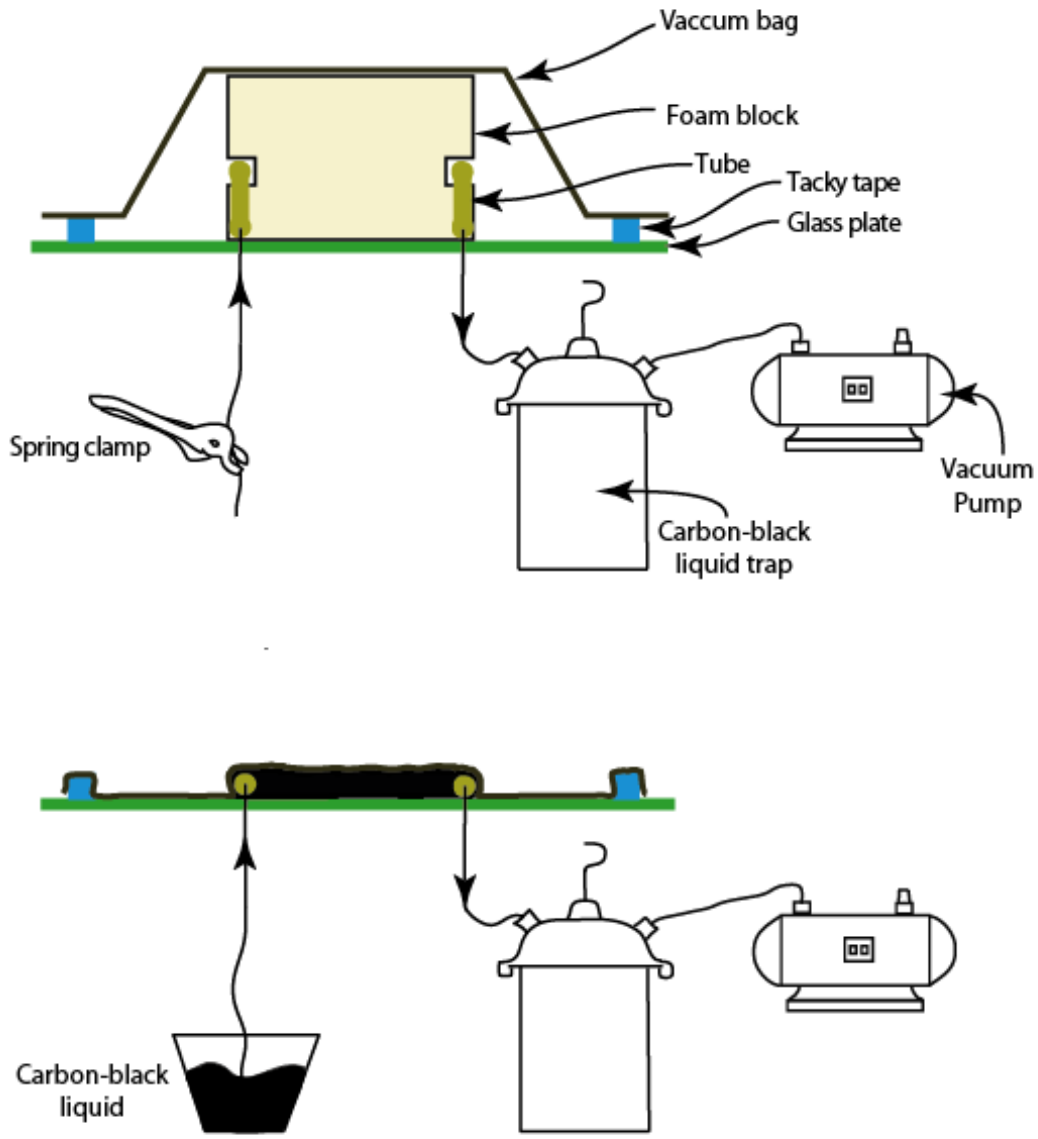

Figure 1.4: Schematic of VAI process

Fig 1.4 depicts the vacuum assisted infiltration process for infiltrating the solution that contains carbon-black and fire retardant salts. During the VAI process, the open cell polyurethane foam is compressed by a powerful suction generated by the vacuum pump. The liquid is then let inside from one side to get dispersed across the sample. Optimum dispersion of the liquid is mainly dependent upon the permeability of the foam which is again governed by the level of compression of the foam exercised by the vacuum power. Therefore it is imperative to determine the foam material parameters for accurate prediction of the foam compression that can further be utilized to predict the permeability of the foam at various compression levels.

1.4 Literature Survey

1.4.1 Foam Material Parameters

Since foams have a structure that is relatively complex than other materials, the resulting mechanical behavior under compression is also complex which makes it difficult to predict accurately. Before the computer aided engineering tools can be used to predict the behavior of foams, they must be expressed mathematically in the finite element software for doing elemental analysis. A commonly used method to find the material parameters is to fit the experimental data to the constitutive equation formulated for the specific type of foam. Constitutive equations have different material parameters and help the general model to be adapted to represent a specific type of foam.

Since the actual performance of foam is highly non-linear in nature, consideration of the simple isotropic linear elasticity for modeling does not yield expected results [14]. Moreover, it is impossible for a simple model to predict the bottoming out phenomenon that is critical to designing foams. As the elastomeric foams fall under the category of hyperelastic materials, their performance can be described using strain energy density function,

Investigator	Application	FE Package	Type	Parameters	Test Data
Erdemir *et al* [7]	Shoe insole	ABAQUS®	Hyperfoam	2nd order	Uniaxial compression, simple shear, and combination of both
Lemmon *et al* [8]	Shoe insole	ABAQUS®	Hyperfoam	3nd order	Uniaxial compression
Ragan *et al* [9]	Wheelchair cushion	ANSYS®	Linear elastic	E = 22 kPa, v = 0.1	Uniaxial compression
Chen *et al* [10]	Shoe insole	MARC	Rubber foam	1st and 2nd order	Uniaxial compression
Dionne *et al* [11]	Wheelchair cushion	Ansys	Linear elastic	NA	Uniaxial compression
Mills *et al* [12]	Cushion	ABAQUS®	Hyperfoam	2nd order	Compression and shear
Lyn, Mills [13]	Crash mat	ABAQUS®	Hyperfoam	2nd order	High strain uniaxial compression

Table 1.1: Literature survey on elastomeric foams

and depends on the material deformation described by three principal stretches ($\lambda_1, \lambda_2, \lambda_3$) or invariants ($I_1, I_2, I_3$). Three dimensional stress-strain relationships can be obtained by taking partial derivatives over strain energy density function with respect to three principal stretches.

Petre $et\ al.$ [15] had come up with an optimization technique that determines parameters for elastomeric foams, using constitutive models by minimizing the error between model predictions and experimental data for mixed loading conditions. Constitutive model was coded in Matlab® and a desired fit was achieved to get material parameters from experimental results. These materials parameters were then used in foam models to simulate the actual experiment using ABAQUS®.

Mills $et\ al.$ [12] had conducted tests and measured response of open cell polyurethane foams in compression, simple shear and combination of all modes. The data was fitted to constitutive equations related to hyperelastic solids that use Ogden's strain energy function. He then compared the Ogden's function with predictions using micromechanics model.

Scanlon $et\ al.$ [16] modeled indentation on bread crumb using finite element analysis. Hyperfoam material model in the ABAQUS® was applied to study the mechanical properties of the crumb of white bread loves. A similar approach of using the uniaxial compression stress-strain data was followed to model the curves by finite element analysis. The crumb's compressive material parameters predicted from the Ogden strain energy function were used in the analysis to correlate the experimental compressive Young's modulus and critical stress.

Literature survey on predicting the material parameters of polyurethane foams is listed in table 1.1.

1.4.2 Permeability

Permeability is of great importance in vacuum assisted infiltration process. In fluid mechanics, the permeability of a porous material is well defined as a measure of its ability to transmit fluid across it. There exists only a limited number of investigations on the permeability of open-cell foams, albeit the hydraulic permeability of open-celled materials has been studied in detail. However, various researchers have been trying to conduct many permeability measurements in compressed open-cell polyurethane foams that mainly use Darcy's fluid field equations as the backbone [17–19].

Dawson $et\ al.$ [20] proposed a permeability model on low-density open-cell foams under compressive strain. Using this model, they developed a tractable relationship between the normalized permeability and the applied strain. They also analyzed the effect of strain on the permeability of open-cell polyurethane foams by conducting an experimental study. It was found that the developed model had a good correlation with the experimental data without having any dependences on the foam cell size, flow direction with respect to the foam rise direction, and the saturating fluid properties. Later the model was combined with Darcy's equation to give the viscous fluid flow contribution to the stress-strain response of foam under dynamic loading.

Annapragada $et\ al.$ [21] proposed a computational methodology to predict the permeability and thermal transport in compressed open-cell metallic foams. Using finite element method, various unit-cell foam geometries were deformed numerically under uniaxial loading. Based on the deformed solid unit-cell geometry, an algorithm was developed to deform the fluid mesh domain inside the unit-cell foam. Direct simulations were performed on the deformed meshes for the fluid flow analysis over a range of Reynolds numbers. A corrected model was proposed for permeability versus strain after validating the simulation against experimental results.

Lusher $et\ al.$ [22] did a study on hydraulic permeability of open-cell hydrophilic polyurethane foams at steady state over a pressure gradient range of 10^2–$10^4 dyn/cm^3$. It was found that the measured permeabilities were sensitive to the relative amounts of surfactant, prepolymer, and water, and to the mode with which these have been prepared. In addition, from the notable variations between sample-to-sample, it was suggested that effects of mixing were significantly present on the permeability. At higher pressure gradient testing range, only a minor factor was observed on the accountability of foam compression towards the decreased permeability. The Darcian permeability values were correlated against cell size using the Carman–Kozeny equation. From the correlation it was observed that the pore size was the major determinant of hydraulic permeability rather than porosity.

1.5 Scope of The Research

Pyramidal shape polyurethane foams fabricated at ETS-Lindgren are being used for Radio-frequency and acoustic shielding applications. The general manufacturing process followed at ETS-Lindgren involves immersion of PU foam blocks in a bath of carbon black solution and fire retardants followed by cutting the blocks into complex pyramidal shapes. Since the immersion process has inbuilt conductivity variation, it impacts the absorption property of the foam.

In addition to the above, a significant overhead cost was incurred due to the large quantity of scrap generated during the process that needed treatment for removing chemical hazards before being disposed into landfills. Thus, the initial scope of the research was to develop a potential alternative for the existing fabrication process that could reduce the total overhead costs, and subsequently improve the electrical conductivity. Hence, a vacuum assisted infiltration technique was developed to infiltrate the solution directly onto the pyramidal foams.

With the VAI on foams as a primary motivation for this research work, the scope of this research is to predict the variation of local permeability that would define the flow characteristics of pyramidal foams under compression during the vacuum assisted infiltration process. This variation in local permeability can be used for predicting fluid flow using computational fluid dynamics in VAI. Modeling the fluid flow would be helpful in predicting the wettability of carbon black fluid on foam and also in locating the inlet and outlet ports of VAI setup to achieve homogenous infiltration. As the infiltration takes place when the foam block is compressed, it is imperative to predict the behavior of foams under compression. Hence, predicting the compression behavior of a non uniform pyramidal foam block and the variation of local permeability of pyramidal foam blocks under compression are the primary subjects of interest for this research work.

CHAPTER 2

FABRICATION

2.1 Current material fabrication technique for manufacturing absorber foams

A solid block of raw polyurethane open-celled foam is initially loaded with carbon black by immersind in a liquid bath of carbon black and dried for 18–20 hours in hot oven. The dried carbon-loaded foam block is then loaded with fire retardants salts and again re-dried for 18–20 hours. The treated foam is then taken to machining process where the block is cut to required shapes. A schematic of the current fabrication technique is shown in fig 2.1

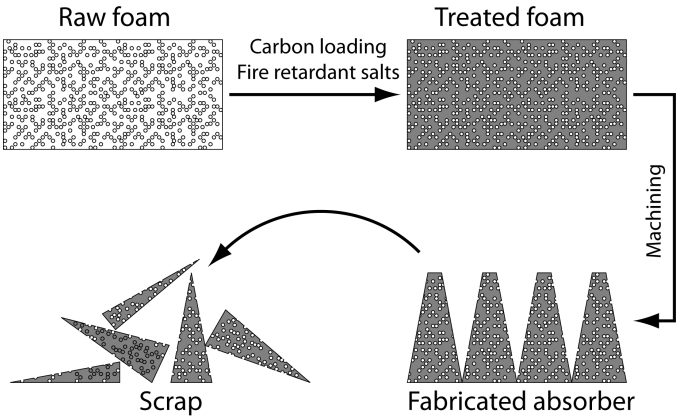

Figure 2.1: Current Fabrication Technique for Absorber Foams [6]

The current manufacturing technique of absorber foams has primary drawbacks of disposal cost which is comprised of two components: the cost of foam-scrap itself, and the cost of back-treatment of the scrap to safeguard the environment from toxic chemicals.

2.2 Vacuum Assisted Infiltration Process (VAI)

Vacuum assisted infiltration process is a potential alternative for the existing fabrication process to reduce scrap and variation in conductivity of foam samples. In the proposed VAI process, the foam is compressed under vacuum before being infiltrated by the carbon-loading liquid or fire-retardant salts. Vacuum is maintained to remove the excess liquid and this process aims at the following:

1. Reduce the carbon black scrap content from the cut solid foam blocks by infiltrating into the final desired shape. This minimizes the resources spent on the chemical treatment of scraps before disposal.

2. Minimize the variation in conductivity of foam blocks infiltrated with carbon black used for RF shielding applications

3. Allow for infiltration of complex shapes whereas the current technique is limited to uncut foam blocks. This would save time, energy, and the wastage of carbon and fire-retardant materials that are currently discarded with cut foam scrap.

2.2.1 Vacuum Assisted Infiltration Setup

Vacuum assisted infiltration, VAI, is a simple and useful technique to infuse fluids into any materials where the primary interest is to make the infusion more homogenous and consistent. In case of absorber foams, this process aids in uniform dispersion of carbon black achieving good distribution of conductivity across the sample. VAI employs the vacuum bag technique, in which the wastage of fluid is much lesser compared to other fabrication techniques.

This method utilizes vacuum to infuse liquids into the subject material. A flexible vacuum bag is placed over the top of the foam and then glued to the vacuum sealing tacky tape spread around the foam block to form a vacuum-tight seal. A vacuum pump or liquid trap

(a) Raw Foam

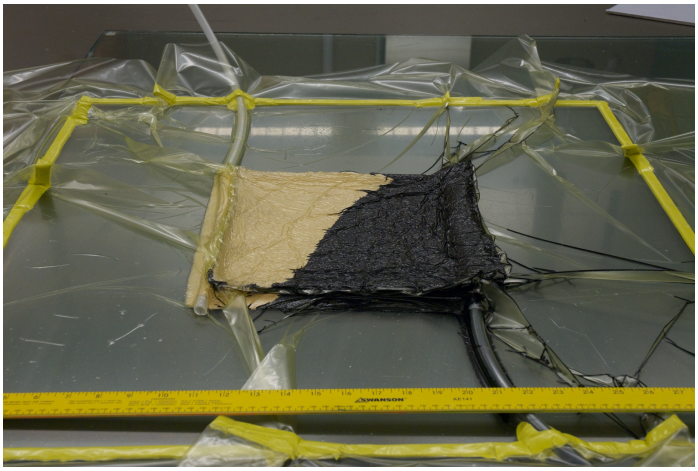

(b) Infiltration

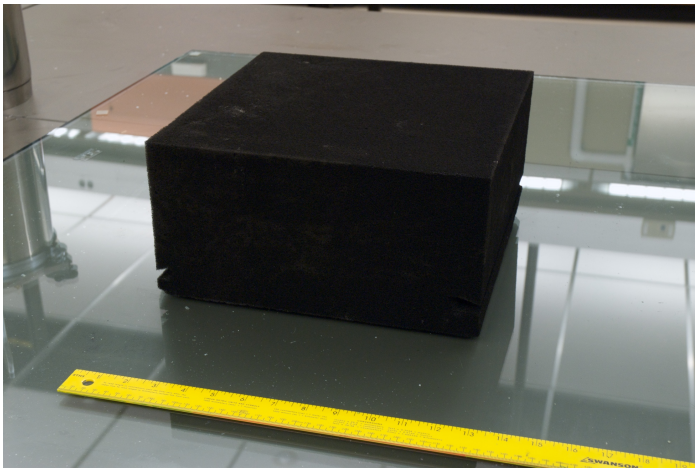

(c) Carbon foam

Figure 2.2: Carbon infusion of foam

is used to evacuate the sealed enclosure. The liquid carbon-black solution is then passed on through the inlet port and gets infiltrated onto the foam by means of the spiral conduits placed inside the groove cut out in the foam block. The carbon black mixture is allowed to pass through the foam for a few minutes until it is completely infiltrated and then, the port is shut off using a spring loaded clamp. The vacuum bagging is then removed and the foam is allowed to dry. A pictorial representation of the process is shown in fig. 2.2

A typical laboratory fabrication is carried out by laying the sealing/tacky tape to a size usually greater than the effective material/infusion area on the top of a glass plate, and the sample (through which carbon-black is to be infused) is placed inside the infusion area. The polyethylene sheet is then stuck from one side and run all the way around. During this lay up, careful attention is given to ensure such that there are no air pockets trapped between the sheet, tape, and the connecting tubes on the inlet and outlet side of the bagging. After ensuring a perfect sealing, the liquid inlet tube end is closed and the pump is switched on to evacuate all the air from the bag. The liquid is now ready to be infused.

In the above conventional procedure, an attempt was made to save time in the bagging/layup process. In this method, instead of gluing the tacky tape initially on the glass plate, it is first glued over the polyethylene sheet to a size just greater than the effective material/infusion area. And, after placing the foam over the glass plate, this sheet with already glued tacky tape is placed directly over the glass plate. This greatly enhances the setup time. Thus the total time of VAI process by this method can almost be reduced by 50% of the total time taken by the conventional layup process.

2.2.2 Determination of Electrical Conductivity and Drying Time

The infusion of carbon black by VAI was carried out on standard foam blocks of dimensions $10" \times 10" \times 5"$. This process was carried out in two sets of three samples each and

the resistance was measured after the carbon black solution was dried completely. The first set of samples were subjected to VAI and then allowed to dry in air at room temperature whereas forced air at room temperature was passed through the inlet tubing for thirty minutes after VAI to accelerate the drying time on the second set.

Resistance values were measured with the distance between the probes maintained constant during each measurement to replicate the measurement technique at ETS-Lindgren. Two values of resistance per side of foam block was recorded which resulted in a total of twelve resistance values for a foam block. The wet weight of the foam blocks were monitored on hourly basis to measure the drying time/quantity of evaporated carbon black. A representation of the measurement method is shown in fig.2.3 below

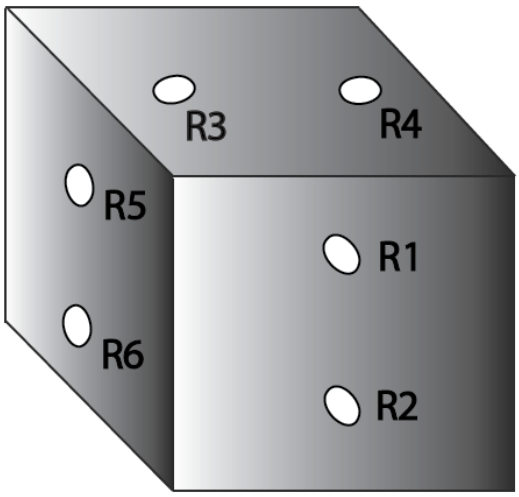

Figure 2.3: Measurement of resistance values

2.2.3 Results and Summary

The measured resistance values on the samples made by VAI were significantly lesser than those values measured on the sample provided by ETS-Lindgren. As resistance is inversely

proportional to conductivity, it implies that lesser the resistance values, better the conductivity. A plot of resistance values of VAI and ETS-Lindgren samples is represented in fig.2.4.

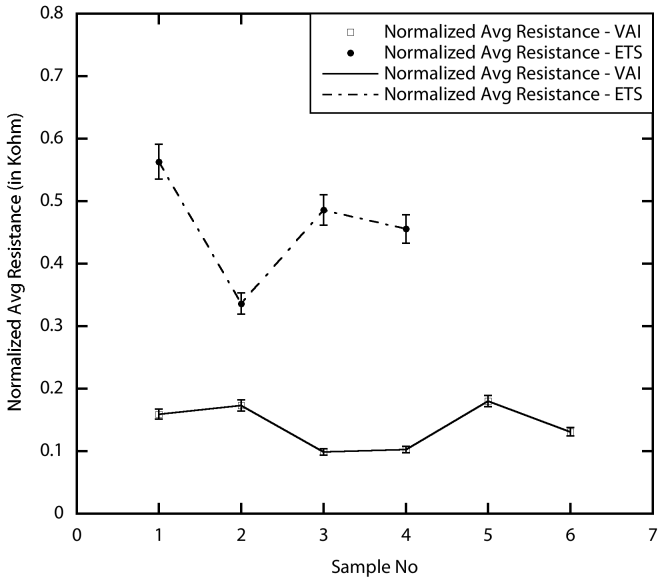

Figure 2.4: Resistance values normalized with arbitrary values

These resistance values were normalized with arbitrary values to protect the data based on our collaborator's interest. It could also be inferred that the distribution of the carbon black mixture was homogenous in those samples prepared by VAI when compared to the direct immersion method. Reduction in the weight of the infiltrated fluid was measured for 30 hours at room temperature to observe the pattern of drying with respect to time as shown in the fig.2.5. It was observed that the samples were not completely dried after the end of 30 hours. An attempt to achieve complete drying was carried out by passing forced air using a portable heat gun for thirty minutes immediately after infiltration. The temperature of the air measured around 100°. There was no significant increase in temperature observed

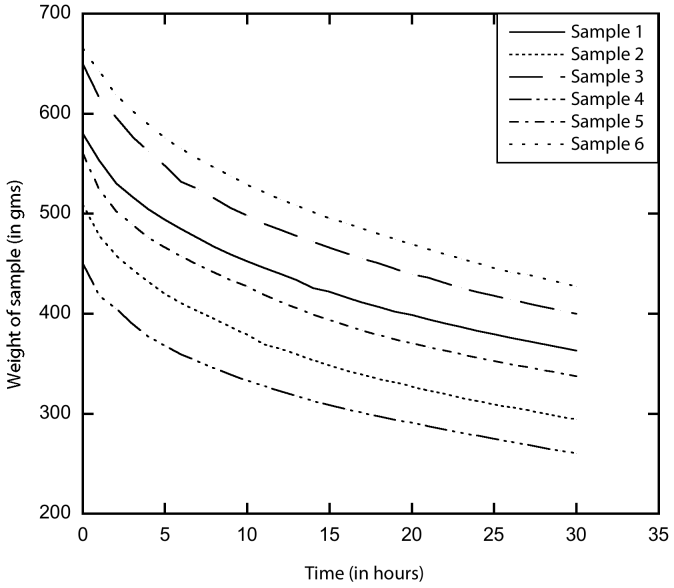

Figure 2.5: Drying time plot at room temperature

inside the vacuum bagging enclosure as the velocity of air from the heat gun was faster than the vaccum generated by the vacuum pump. Another approach was attempted by connecting the inlet tubing with thermal insulations into the exhaust pipe of hot oven where the outgoing hot air measured about 120°. The tubing was placed this way for thirty minutes but the attempt proved futile as no significant increase in temperature was observed.

However, this could be improved by passing the infiltrated foam blocks through a chamber of hot air in conveyors. Also, reduction in relative humidity might help in solving the problem to a certain extent.

CHAPTER 3

EXPERIMENTATION AND SIMULATION

3.1 The Approach

This chapter explains the approach followed in predicting the foam permeability using evaluated material parameters, experimental procedures, and simulations carried out in ABAQUS®.

The flow of fluids through compressed open cell foams has been well studied in the last few decades. The primary relation for the pressure gradient required to maintain fluid flow at a velocity v through a porous medium can be resolved into two terms [23, 24] and is represented by

$$\frac{\Delta p}{L} = \frac{\eta}{K} v + \frac{\rho}{B} v^2 \tag{3.1}$$

where η and ρ are viscosity and density of the fluid, respectively. The foam permeability, $K(m^2)$, and the inertial flow coefficient, $B(m)$, are the coefficient characteristics of the medium. Hilyard and Collier (1987) related these constants B and K, as a function of compressive strain for various open cell foams. They extended the prediction and related the first term on the right hand side of the equation (3.1) to laminar air-flow and attributed the second term to flow by inertial forces.

As B and K are crucial in predicting the flow characteristics through porous media, it is of our prime interest to evaluate these parameters in a process like vacuum assisted infiltration. With the confidence obtained from initial VAI trials, this study was focused on

predicting the flow coefficients which would form as a primary reference for flow analysis and simulation when carried out on a larger scale. A pyramidal geometry is considered for our work and it will have a significant variation in strain along it's length under compression. As permeability and inertial flow coefficient is related to strain, it is of our prime interest to predict these strain contours. The first step in this procedure is to evaluate the material parameters for modeling the behavior of polyurethane foams under uniaxial compression.

Linear-elastic models are not best suited for describing the large strain response of flexible foams — if a compressive stress equals the Young's modulus, it would cause the height of a block of such foam material to decline to zero level — whereby, theoretically, an infinite foam-density is obtained which is physically impossible [14]. Hence, there should exist a non-linear stress-strain relationship that could increase the slope of the curve with increasing compressive strain values of foam. If the time-dependent mechanical properties and hysteresis are ignored, they can be approximated as hyperelastic solids or hyperfoams. Nonetheless, in polyurethane foams, efforts to uncover the elastic response during the large strain compression have failed, and consequently, any elastic model is an approximation. Hence, an appropriate relation for strain energy function U can be formed and the parameters can be determined from the stress and principal extension ratios λ_i [14].

$$\sigma_i = \frac{\partial U}{\partial \lambda_i} \tag{3.2}$$

The material parameters were found by fitting the Ogden's constitutive model with the uniaxial compression experimental data. Simulation of uniaxial compression on pyramidal foam blocks using ABAQUS® and prediction of permeability from the strain contours was also carried out.

3.1.1 Uniaxial Compression Testing of Cubical Foam Blocks

The first step in evaluating the material parameters of the foam blocks was initiated by finding the stress strain response under uniaxial compression. Uniaxial compression testing was conducted on virgin and carbon loaded polyurethane foams. Three samples of size 50mm $\times$ 50mm $\times$ 50mm of each type of foam block were tested and they were pre-flexed before compression [25]. Compression testing was carried out in Instron (model 5581) to get the stress-strain response from cubical foam blocks, as shown in fig. 3.1. The load–displacement data were then used to establish the required stress-strain plot.

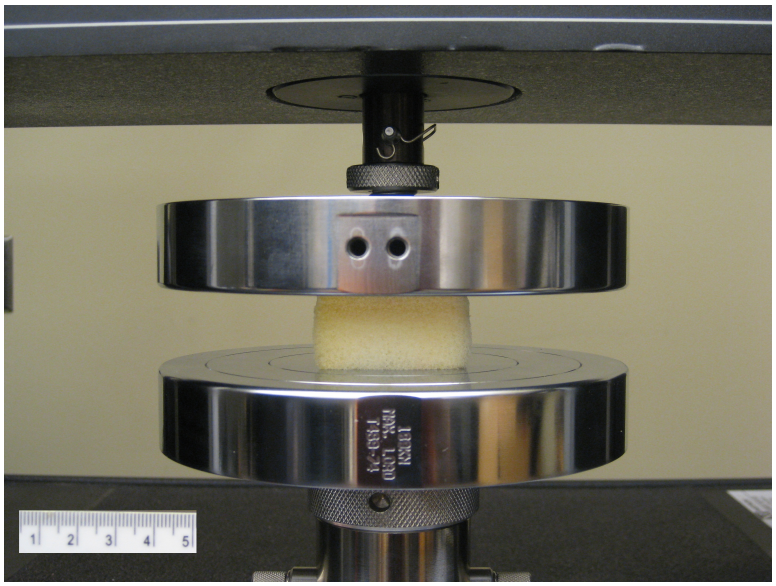

Figure 3.1: Open-cell foam under compression

The stress-strain plot of a foam in compression can be subdivided into three distinct regions as shown in figure3.2. The first region is linear elastic where the cell walls or struts experience bending, the secondary region is a plateau where unfavorably oriented cells buckle and collapse, and the tertiary region is the densification zone where severe stiffening occurs due to the compaction of the foam [26]. The densification region is characterized by crushing of the cell walls which results in a significant increase of stress for a small increment of strain. In open-celled foams, volumetric compression is mostly dominated by

buckling of struts.

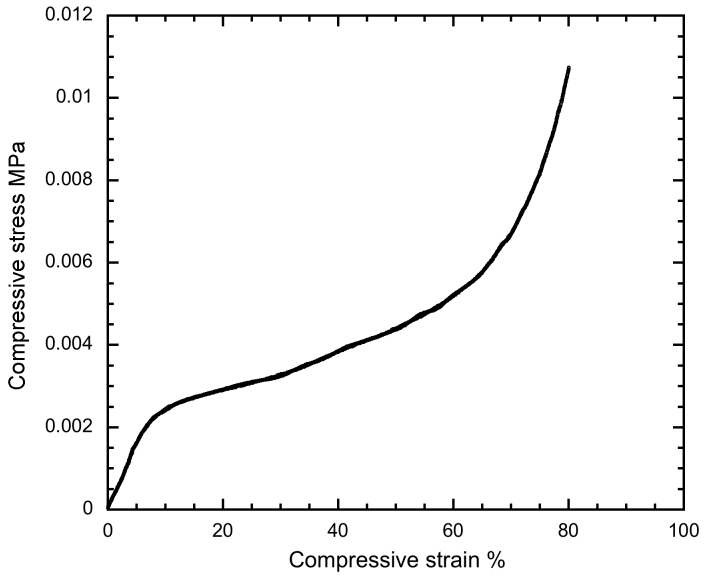

Figure 3.2: A typical stress-strain plot of a open cell polyurethane foam under compression

At higher compressive strains, the foam structure collapses and exhibits a phenomenon called bottoming out, beyond which localized pressure is exerted. In the event of prolonged usage, the mechanical property of foams slowly start compromising and the likelihood of bottoming out increases. This may be due to the damaged struts or cell walls.

3.2 Foam Material Parameters

3.2.1 Ogden model–A Strain Energy Approach for Compressible Elastomeric Foams

In 1972, Ogden proposed a strain energy function for slightly compressible rubbers that contained strain variants and integral powers [27]. Subsequently, it has been adapted for low density highly compressible foams. The modified Ogden-Hill strain energy potential equation for elastomeric foams is available in the commercial finite element analysis (FEA) software, ABAQUS® [28] under the material model Hyperfoam.

From the ABAQUS® users manual, the strain energy potential function for Hyperfoam material can be found as,

$$U = \sum_{i=1}^{N} \frac{2\mu_i}{\alpha_i^2} \left[(\lambda_1^{\alpha_i} + \lambda_2^{\alpha_i} + \lambda_3^{\alpha_i} - 3) + \frac{1}{\beta_i}(J^{-\alpha_i \beta_i} - 1) \right] \tag{3.3}$$

where,

λ_i are the principal stretches,

J, the measure of the relative volume,$= \lambda_1 \lambda_2 \lambda_3 = \sqrt{I_3}$,

μ_i is the shear moduli,

N is an integer,

α is the material parameter,

β is the foam compressibility coefficient.

Here the deformation modes are captured through three principal stretches and volumetric strain, J. As the elastomeric foams are highly compressible materials, $J = \lambda_1 \lambda_2 \lambda_3 \neq 1$. The coefficient β_i that determines the compressibility is related to Poisson's ratio v_i by

$$\beta_i = \frac{v_i}{1 - 2v_i}$$

In order to ensure stability, it is necessary that

$$\beta_i \geq -\frac{1}{3}$$

The term μ_i is related to μ_0, the initial shear modulus, by the expression

$$\mu_0 = \sum_{i=1}^{N} \mu_i$$

The initial bulk modulus, κ_0

$$\kappa_0 = \sum_{i=1}^{N} 2\mu_i \left(\frac{1}{3} + \beta_i \right)$$

The value of N, or order, can be integers from 1–6. The choice of N value is based on the degree of non-linearity and the available test data for predicting the material parameters. The order of N increases when multiple test data from compression, shear, and volumetric response are used. However, a lower order of N will normally fail to capture the non-linearity with required accuracy for samples which has significant effects under different loading [29]. Thus, the typical N value would be 2 or 3 for which a minimum of 50% compressive strain is exercised.

3.2.2 Determination of Material Parameters from Stress Strain Response

The strain energy potential function for elastomeric foam materials is driven by three important parameters, namely, $\mu_i, \alpha_i,$ and β_i. Stress-strain relationships for different types of loading — uniaxial, simple shear, and combination, are determined by partial derivatives of the strain energy potential function with respect to three principal stretches. This work primarily focuses on uniaxial compression following the pedigree of other research on low density polyurethane foams and soft biological tissues which are characterized by the Ogden's material model as they exhibit similar nature like elastomeric foams. Hence the stress-stretch($\sigma_i - \lambda_1$), relationship is obtained from the partial derivative of strain energy(U) over stretch in the uniaxial deformation, λ_1. This relationship was then incorporated into Matlab® and fitted with the stress-strech response to determine the three material parameters: $\mu_i, \alpha_i,$ and β_i.

3.2.3 Stress(σ)−Stretch(λ) from Ogden's Strain Energy Potential

In uniaxial compression, since lateral stretches were not measured during the test and uniaxial stress is a function of volume strain, $J = \lambda_1\lambda_2\lambda_3$, the lateral stretches were determined in terms of uniaxial stretch, λ_1, through the material's compressibility parameter, β, by applying the zero lateral stress constraint [30–34].

Thus, relation between stretches can be written as

$$\lambda_T = \lambda_2 = \lambda_3 \tag{3.4}$$

$$= \lambda_1^{\frac{-\beta}{1+2\beta}} \tag{3.5}$$

Volumetric strain, J

$$J = \lambda_1\lambda_2\lambda_3 \tag{3.6}$$

$$= \lambda_1 \times \lambda_1^{\frac{-\beta}{1+2\beta}} \times \lambda_1^{\frac{-\beta}{1+2\beta}} \tag{3.7}$$

$$= \lambda_1^{1+\left(\frac{-\beta}{1+2\beta}\right)+\left(\frac{-\beta}{1+2\beta}\right)} \tag{3.8}$$

$$= \lambda_1^{1-\frac{2\beta}{1+2\beta}} \tag{3.9}$$

$$= \lambda_1^{\frac{1}{1+2\beta}} \tag{3.10}$$

The applied stress for uniaxial compression along the first axis is obtained by differentiating the strain energy density function with respect to the stretch in the direction of deformation.

$$\sigma_1 = \frac{\partial U}{\partial \lambda_1} \tag{3.11}$$

$$= \frac{2}{\lambda_1} \sum_{i=1,n} \frac{\mu_i}{\alpha_i} (\lambda_1^{\alpha_i} - J^{-\alpha_i\beta_i}) \tag{3.12}$$

$$= \frac{2}{\lambda_1} \sum_{i=1,n} \frac{\mu_i}{\alpha_i} (\lambda_1^{\alpha_i} - \lambda_1^{\frac{-\alpha_i\beta_i}{1+2\beta_i}}) \tag{3.13}$$

$$= 2 \sum_{i=1,n} \frac{\mu_i}{\alpha_i} (\lambda_1^{\alpha_i-1} - \lambda_1^{\frac{-\alpha_i\beta_i}{1+2\beta_i}-1}) \tag{3.14}$$

$$= 2 \sum_{i=1,n} \frac{\mu_i}{\alpha_i} \left[\lambda_1^{-(1+\alpha_i)} - \lambda_1^{-\left(1+\frac{\alpha_i\beta_i}{1+2\beta_i}\right)}\right] \tag{3.15}$$

3.2.4 Curve Fitting in Matlab®

The stress(σ)$-$stretch(λ) response of hyperfoam material model under uniaxial compression derived in the equation 3.15, was incorporated into Matlab® (Version R2010a) curve fitting tool. Experimental data from the uniaxial compression test with negative strain in

compression is converted to stretch by the relation, $\lambda = (1 + e)$ [35]. A curve fit operation was performed by fitting second order of Eq (3.15) to the experimental data specified as nominal stresses and nominal stretches. The material parameters were solved by minimizing the error between the predicted model and experimental values.This was done by the nonlinear optimization technique following a nonlinear least-squares-approximation method in Matlab® [36].

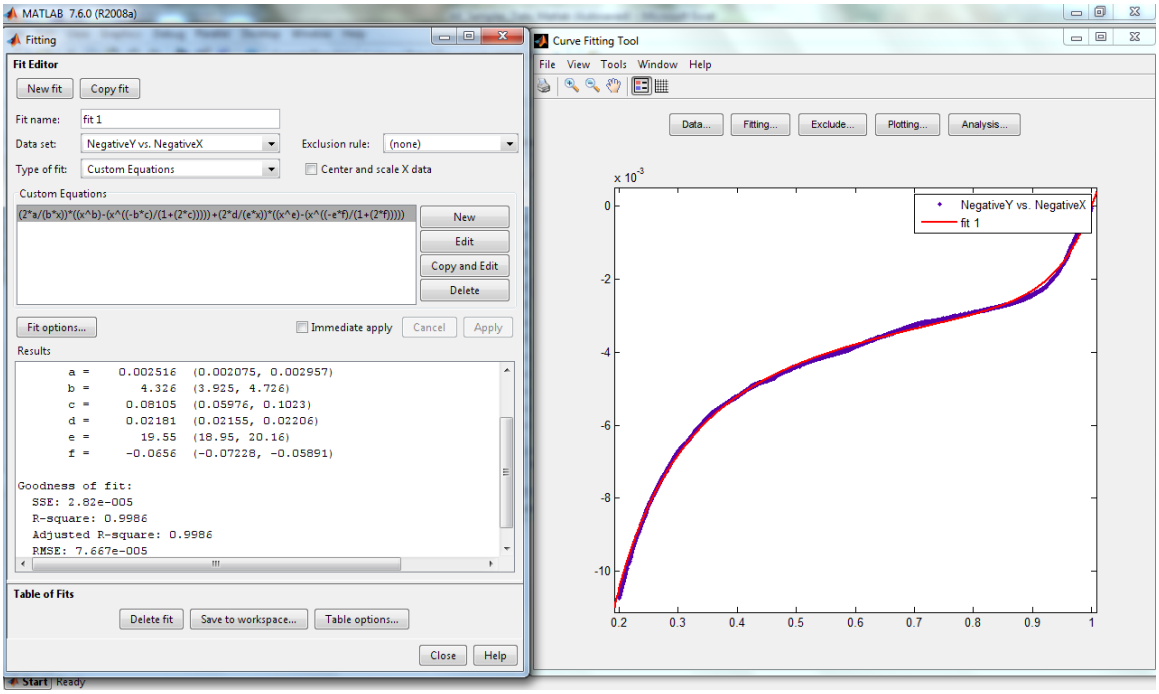

Figure 3.3: Curve fitting of polyurethane foam experimental stress-stretch in Matlab®

The Trust-Region algorithm was chosen, which is claimed to be more powerful than Levenberg-Marquardt and Gauss-Newton algorithms for a non-linear curve fitting procedure [37]. The lower and upper limits were adopted from Petre et al's work and the bounds were fixed at [-10,10] Mpa for μ_1 and μ_2, [-50,50] (unitless) for α_1 and α_2, and [-0.3,1] (unitless) for β_1 and β_2 respectively. As the optimization process fits the curve to attain the least root mean square in order to provide the best fit, it is possible that the predicted values might exceed the realistic value of these parameters. It is also possible that the same curve could be fit with a very close RMS error but with extremely different material pa-

rameters. Hence, the optimal curve fit was performed to attain positive values for shear modulus $\mu_1 and \mu_2$, as no physically realistic deformation would result in a negative shear modulus. α_1, α_2 were not allowed to be zero for numerical stability and β_1, β_2 were restricted within [-0.3,1](unitless) to reflect the nature of highly compressible foams [38]. A set of material constants/parameters were obtained for raw foam and carbon-black-loaded foams by performing the curve fitting procedure.

3.3 Simulation Technique Using ABAQUS®

3.3.1 Validation of Material Parameters on Cuboidal Foam Blocks

The material parameters predicted using Matlab® must be verified using ABAQUS® before they can be extended to model the compression on the pyramidal foam blocks. This was carried out by reproducing the uniaxial compression on a cuboidal foam block in ABAQUS®. A quarter size of the actual experimental block was modeled for reducing the computation time. A cuboidal block of size 25mm x 25mm x 50mm was modeled. The material parameters were incorporated in the Hyperfoam material model using the coefficient input mode in the property module of ABAQUS®. A dependent part instance was created in the assembly module and the non-linear geometry (NLGEOM) was enabled considering large displacements.

Vertical translation and all rotations were arrested in the bottom face of the block and a negative displacement of 40mm was defined on the top face of the foam block. Rectangular meshes of size 2.5mm were created in the meshing module. Simulations were carried out with evaluated material parameters for one sample of raw polyurethane foam block and one sample of carbon black infused foam block. The samples were selected by comparing the RMS error and one best fit sample with least error value was selected from each category. The results of the stress(S22) vs strain(LE22) were obtained from the visualization module and this image was superimposed with the experimental stress-strain curve. A closer fit

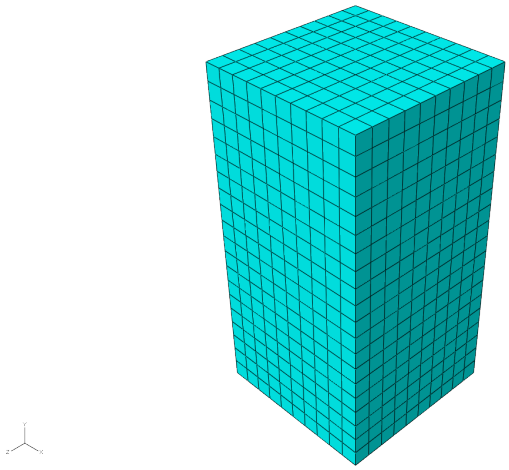

Figure 3.4: Meshed cuboidal block subjected to uniaxial compression in ABAQUS®

from the ABAQUS® results with the experimental curve validated the accuracy of the predicted material parameters.

3.3.2 Simulation on Pyramidal Foam Blocks

Once the material parameters were validated from the uniaxial compression of cuboidal foam block, it was then extended to model compression on a scaled down acoustic absorber foam block. A block of foam, 1/64th in size of an absorber foam block obtained from ETS-Lindgren was modeled in Solidworks 2010® with four pyramids rested on a rectangular base. Each pyramid of height 62.5mm was modeled and an array of four pyramids of same dimensions were created on the top of a rectangular base measuring 37.5 x 37.5 x 12.5mm. This was exported as a initial graphics exchange specification (IGES) file for performing compression simulation in ABAQUS®. The imported model was then assigned suitable material parameters using the Hyperfoam material model in ABAQUS® for both raw polyurethane foam blocks and carbon infused foam blocks. In order to carry out an uniaxial compression on a pyramidal foam block, an analytically rigid plate of 75mm x 75mm was modeled and assembled to be in contact with the sharp edges at the apex of the pyramids. Dependent instances were created for both the pyramidal block and rigid plate

in the assembly module. Non-linear geometric parameter(NLGEOM) was enabled considering large displacements. As this problem involves a sharp contact on a material like an elastomeric foam, an adaptive stabilization was used with a maximum ratio of stabilization to strain energy as 0.4 in the step module.

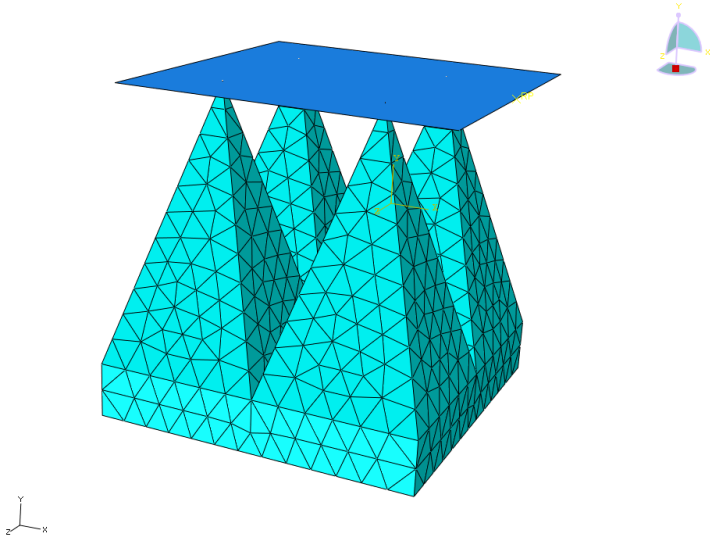

Figure 3.5: Meshed pyramidal block with rigid plate subjected to uniaxial compression in ABAQUS®

Considering the non-linearity of the problem, the maximum number of increments was raised to 10000 with a minimum increment size of 10 $\times 10^{-6}$. The solution technique followed the contact iterations algorithm and conversion of severe discontinuity iterations was turned on to ensure the progress of analysis in the region of severe discontinuities. The rectangular base at the bottom was arrested for all translations and rotations. A negative vertical displacement of 60mm was applied at the reference point of the rigid plate with other translations and rotations arrested in this location. A frictional coefficient of 0.2 was assigned at the point of contact and the interaction is defined by selecting the rigid plate as the master surface and all the pyramids as the slave surface. The pyramidal foam block was meshed as a tet element with a size of 4mm and the rigid plate was left unmeshed. Simulations were then performed and the strain contour plots after compression were ob-

tained from the visualization module. The local logarithmic strains at different regions of the strain contour plots were converted to local engineering strains which was used in the prediction of permeability and inertial flow coefficient across the compressed foam block.

3.4 Determination of Permeability

3.4.1 Strain Dependent Permeability

Hilyard and Collier (1987) showed that, for several types of polyurethane foams, the foam permeability $K(m^2)$ and inertial flow coefficient $B(m)$ were functions of the applied compressive strain. Based on an approximate model for the permeability of isotropic porous solids, they have proposed semi-empirical equations for $K$and B with compressive strain in a direction perpendicular to the flow direction. The relation was obtained from a set of strain measurements ε, 0%–70%, in 50 mm cubic samples.

Inertial Coefficient

$$B = B_0 \left[\frac{1 - \varepsilon - R}{(1 - \varepsilon)(1 - R)} \right]^3 (1 - \varepsilon) \tag{3.16}$$

Strain-dependent Permeability

$$K = K_0 \left[\frac{1 - \varepsilon - R}{(1 - \varepsilon)(1 - R)} \right]^3 (1 - \varepsilon)^2 \tag{3.17}$$

where,

$$K_0 = \frac{d^{2.08}}{215} \tag{3.18}$$

$$B_0 \approx d \tag{3.19}$$

where K_0 and B_0 are the initial permeability and inertial flow coefficients of the undeformed test samples before compression. Hilyard and Collier showed that K_0 and B_0 varied with the mean cell diameter of foams. The relative density (R) is the ratio of weight

density of foam test block(ρ^*) to that of the solid from which the cell walls are made (ρ_s). The solid density(ρ_s) is a standard property for different types of foams and this value for commonly used polymers are available from many resources. Solid density(ρ_s) for flexible polyurethane foams has been inferred as $1200Kg/m^3$ from Cellular solids by Gibson and Ashby [4]. When the foam block was subjected to compression, it leads to densification and the relative density varied with respect to the amount of compression. Hence for a sample with non-uniform geometry like pyramid, it was more accurate to calculate the relative density based on the strain experienced at a particular level of compression instead of calculating the foam density based on reduction in area. Dawson et al, established a relation for relative density (R) with respect to strain, where strain is taken as a negative value in uniaxial compression and represented as

$$\frac{\rho^*}{\rho_s} = \frac{\rho_0^*}{(\rho_s)(1+\epsilon)(1-\nu\epsilon)^2} \tag{3.20}$$

Here ρ_0^* is the initial density of the foam at 0% compression, ρ^* is the density of foam at strain ϵ and ν is the effective poisson's ratio of the foam. Hence, the variation of relative density with different level of strain was obtained from this relation which was used in the equations (3.16 and 3.17) for finding the permeability and inertial flow coefficient.

3.4.2 Determination of K_0 and B_0

It was found that the initial permeability of the uncompressed foam block (K_0) and the initial inertial flow coefficient (B_0)varied with respect to the mean cell diameter (d) of foams. Hilyard and Collier observed that though there were variations in the cell shape and structure of different samples, it was the mean cell diameter that primarily governs the permeability in an uncompressed foam block. Hence, finding the mean cell diameter was important to determine (K_0) and (B_0). The mean cell diameter was found by averaging the minimum and maximum diameters of different cells measured under the scanning electron

microscope (SEM) [39–41].

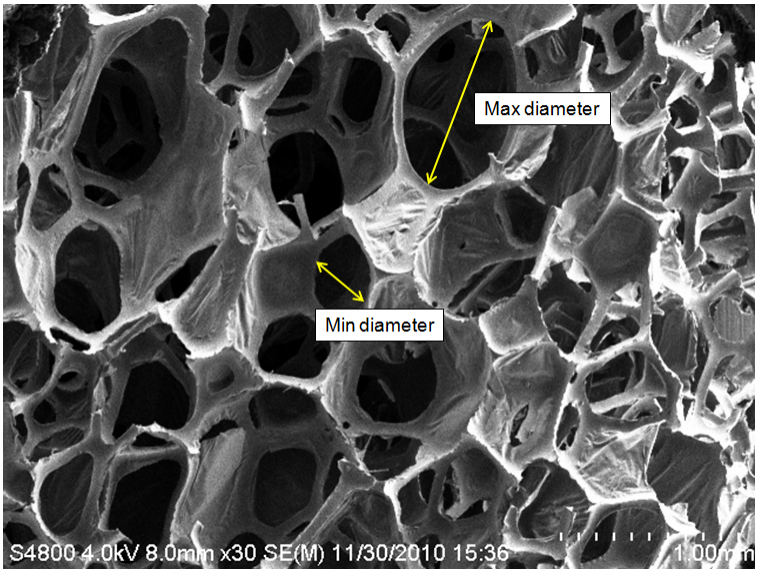

Figure 3.6: Minimum and maximum diameter of foam cells under SEM

The cells were focussed at 1mm resolution obtained by applying a voltage of 4.0kV in the S4800 model of SEM manufactured by Hitachi. The measurements were arrived from whole cells. Abnormally bigger cells were not considered for measurement as they were cut out by the border of the SEM image. The diameters were measured using the ruler tool in the analysis tab of Adobe Photoshop®. At least 20 measurements were made for both minimum and maximum diameters from different SEM images captured from different regions of the foam block. These were then averaged out and the final value was used in the prediction of initial permeability and inertial flow coefficient (K_0) and (B_0) using equations (3.18 and 3.19)

CHAPTER 4

RESULTS AND DISCUSSION

4.1 Compression Model of a Simple Cuboidal Foam

4.1.1 Material Parameters from Matlab®

Experimental stress-stretch curve of raw polyurethane and carbon-black foam was fitted to Ogden's constitutive model for stress-stretch from Eq 3.15 using Matlab®. The best fit was obtained for finding all the foam material parameters by minimizing the error between model predictions and experimental results. From the curve fitting, root mean square errors as a percentage of maximum stress were produced, and a best fit was achieved for each sample that had the least RMS value. Equation 4.1 relates the expression for finding RMS value for each tests done.

$$RMS = \frac{\frac{\sum^{n}(\sigma_{mod}-\sigma_{exp})^2}{n}}{\sigma_{max}} \times 100 \tag{4.1}$$

where,

n is the number of data points being fit,

σ_{mod} is the model predicted stress,

σ_{exp} is the experimental stress,

σ_{max} is the maximum experimental stress.

Curve fitting of second order stress-stretch relationship obtained from Ogden's strain energy potential were performed and the starting points were provided based on the material parameters obtained by Eredemir et al.

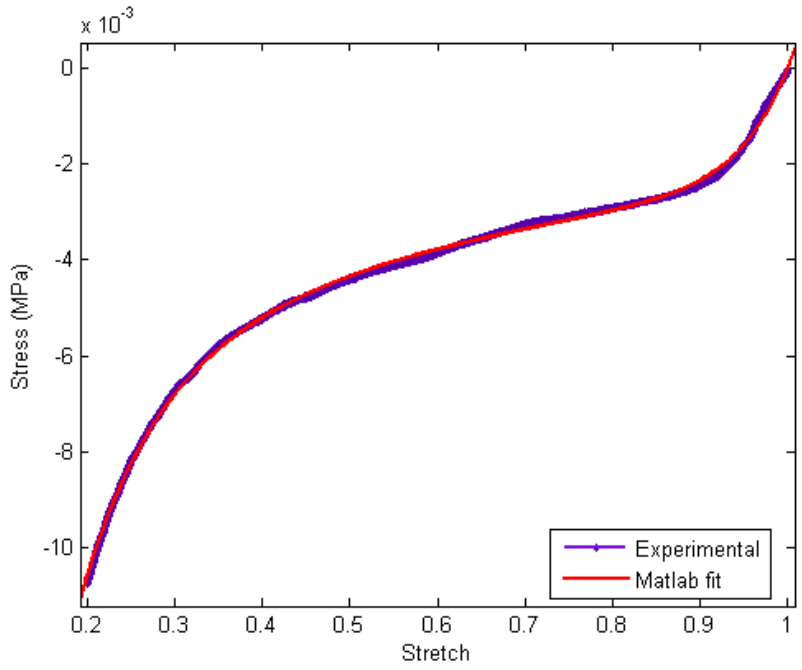

(a) Stress-stretch plot of polyurethane foam

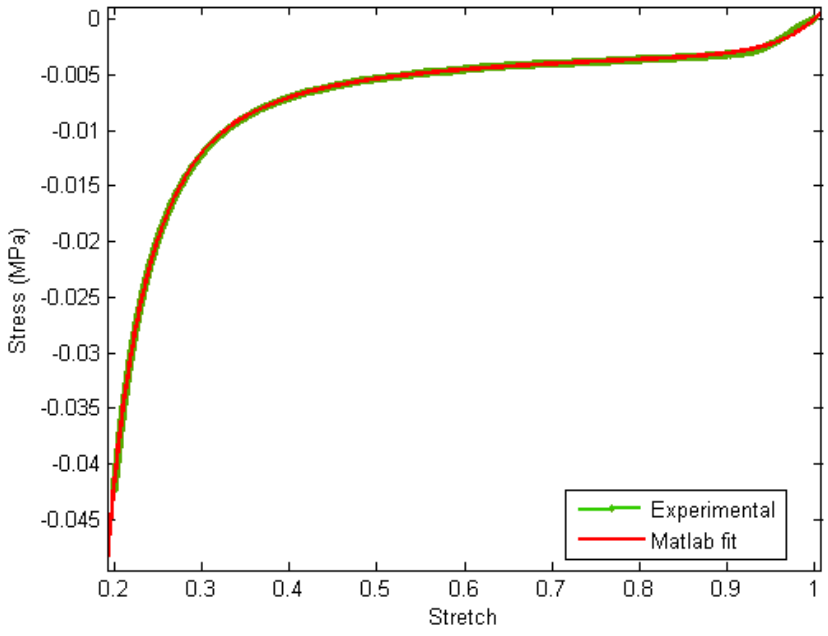

(b) Stress-stretch plot of carbon-black infused polyurethane foam

Figure 4.1: Matlab® fit against experiemental data for 2nd order

Table 4.1 lists the parameters for raw polyurethane and carbon-black foams. Graphs, (a) and (b), of fig. 4.1, represent the fitness of model-predicted stress-strain curve against the experimental data in Matlab® for one sample of raw polyurethane and carbon-black infused polyurethane foam respectively. The compression behavior of raw polyurethane foam suggests that there was a longer initial elastic region and a moderate uptrend in stress in the plateau region followed by densification. Whereas, the carbon-black infused foam was characterized by a shorter elastic region and a perfect plateau region followed by a sharp densification.

Parameter	Polyurethane			Carbon-black		
	Sample 1	Sample 2	Sample 3	Sample 1	Sample 2	Sample 3
μ_1	0.001851	0.002516	0.001233	2.92E-05	4.39E-05	0.0001018
α_1	5.069	4.326	5.143	−4.59E+00	−3.459	−2.467
β_1	0.1154	0.08105	0.1876	0.07889	0.1385	0.107
μ_2	0.02115	0.02181	0.02347	0.03391	0.036	0.04237
α_2	17.75	19.55	19.48	22.19	22.89	20.8
β_2	−0.05694	−0.0656	−0.04439	−0.008637	−0.01583	−0.01702
RMSE	7.03E-05	6.55E-05	7.67E-05	9.97E-05	8.94E-05	9.23E-05

Table 4.1: Matlab® parameters of polyurethane and carbon-black foams

4.1.2 ABAQUS® Simulation Results

A cuboidal shape of foam of one-fourth the size ($25 \times 25 \times 50$ mm) of the actual tested sample was modeled in ABAQUS® to reduce the computational time. The values obtained from ABAQUS® simulation were plotted against the experimental values for the best fit material parameters obtained from Matlab®. The stress strain response obtained from ABAQUS® showed a good match with experimental results with overlapping of the

curves in the initial elastic and plateau region which widens a bit in the tertiary region. This validated the accuracy of the predicted parameters from Matlab® which could be used for modeling the pyramidal foam block. Figure 4.2 shows the ABAQUS® fit against experimental values for polyurethane and carbon-black foam samples.

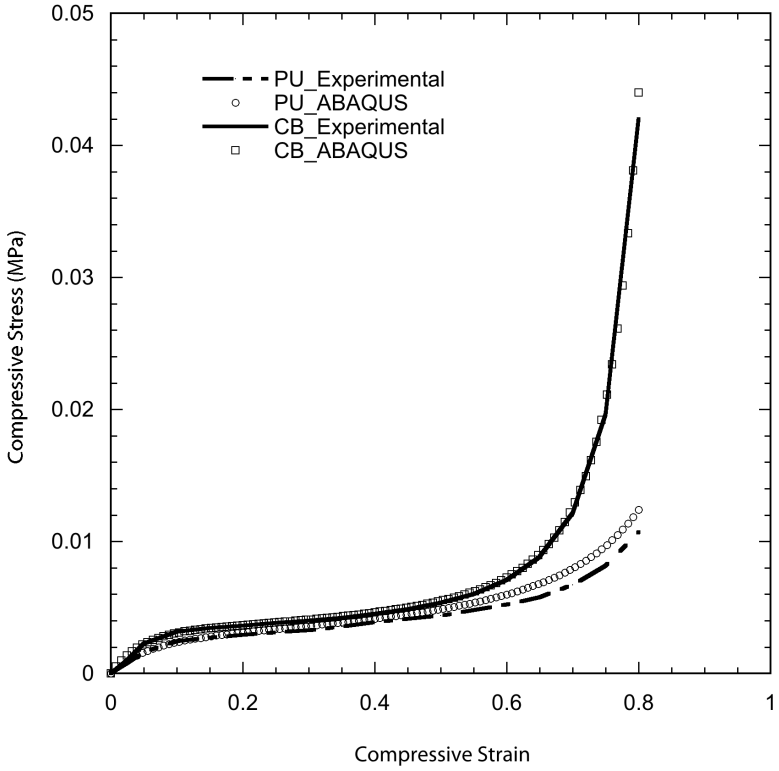

Figure 4.2: ABAQUS® simulation versus experimental data

4.2 Compression Model of a Pyramidal Foam

Finite element simulations on raw polyurethane and carbon infused pyramidal foam block were carried out with the material parameters validated by the cuboidal foam block in ABAQUS®. Strain contour plots were obtained from the Step/frame field output values under the results tab of the visualization module in ABAQUS®. Raw polyurethane foam model under compression exhibited very high local strains near the apex or the edge of the pyramid which were in close proximity with the rigid plate. The distribution of local strain

values along the height of any cross section of the foam block decreased from top to bottom of the pyramid and this pattern was uniform across the width in case of a raw polyurethane foam. The sharp tip at the edge of the foam block was the zone subjected to maximum local strain and proximal locations to the tip experienced relatively lower strains in this case. A contour plot of local strains of the raw polyurethane foam under compression is presented in the figure 4.3

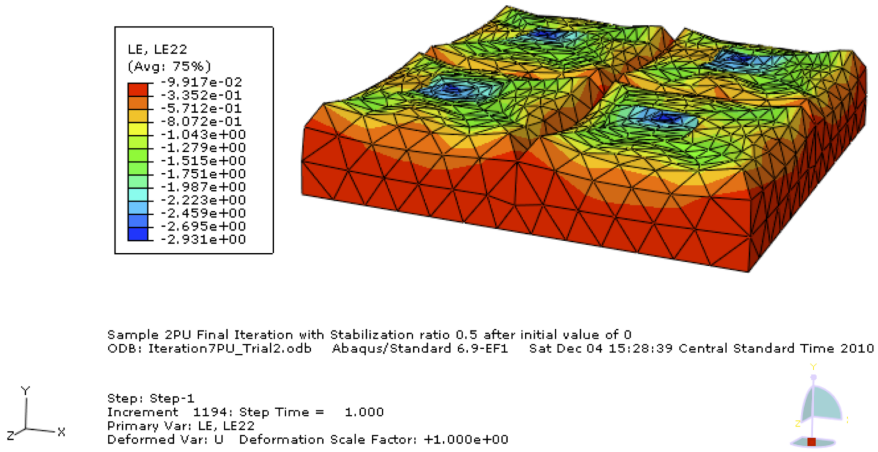

Figure 4.3: Strain contour of compressed raw polyurethane foam

Alternately, running the FE simulation with parameters of the carbon black infused foam showed a distributed pattern of local strains throughout the compressed pyramidal block. The variation of strains were more distributed in this case along the width and height of the foam block. This could be mainly attributed to the higher density of the carbon foam block when compared to the raw polyurethane foam which has made the carbon black foam more stiffer under compression. Higher the density would essentially result in less deformation. A contour plot of strains of the carbon black infused foam is represented in the figure 4.4

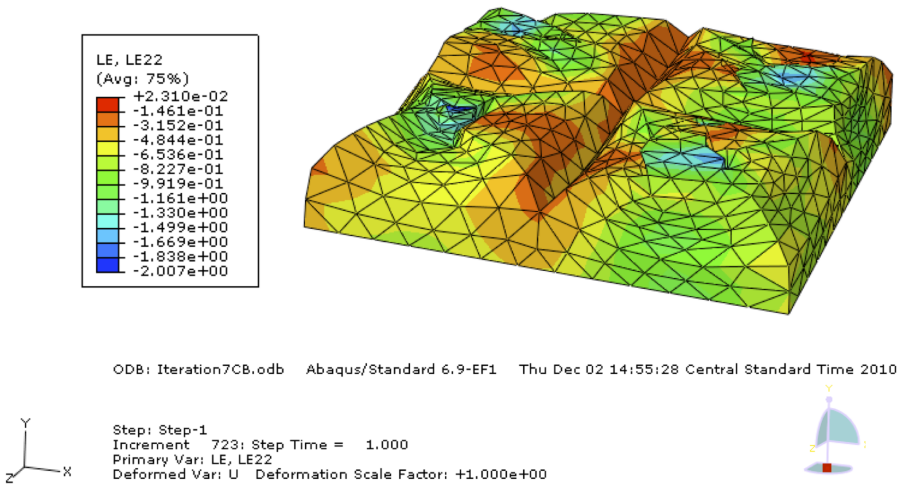

Figure 4.4: Strain contour of compressed raw carbon black infused foam

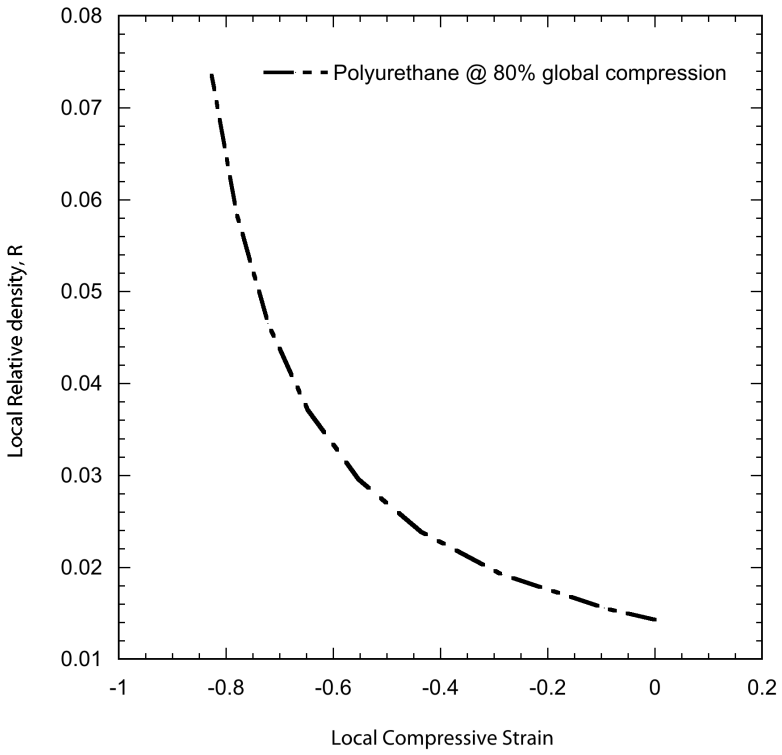

Figure 4.5: Local relative density of polyurethane foam

4.3 Permeability and Inertial Flow Coefficient

The compressive strain values at 80% of the total height of the foam block from ABAQUS® simulation on the pyramidal foam block was used to find the foam permeability related with local strain. Since the relative density (R) of foam is a function of strain, a plot was generated for polyurethane foam in order to observe the variation of R at different regions of compression. Figure 4.5 shows the graph plotted between relative density and local strain. It was observed that the relative density increases with increase in local strain and hence, we can observe the progression of relative density from the bottom face to the top face of the compressed pyramidal block.

The mean diameter of the open cell polyurethane foam was found to be 0.45mm from the average measurements of minimum and maximum diameters. The initial permeability (K_0) and the inertial flow coefficient (B_0) was found to be 5.0844 $\times$ $10^{-10}m^2$ and 4.5 $\times$ $10^{-10}m$ respectively.

From the strain contour plots of raw polyurethane foam, it could be observed that the strain variation from top face to bottom face of the raw PU foam decreases and this is due to the loose nature of the structure; upper half portion of the initial pyramid is strained higher than the remaining part. At locations near the apex, very high local strains ($> 90\%$) lead to negative permeability. This is because the combined value of strain and relative density exceeded the numerical value 1. Obtaining a negative permeability is practically unrealistic. Hence, this indicates that for a particular geometry like a pyramid built with certain material parameters like that of raw polyurethane foam, the compression should ensure that the local strains should not exceed (90%). A generalization that could be arrived is that the combined value of strain and relative density shouldn't exceed the numerical value 1 for having any medium permeable to flow. With respect to strains, it could not be concluded that any block of foam should not be strained higher than 90% of local strain, as it depends

on geometry and also the material density.

In the case of carbon-black infused foam, due to the relatively higher density and higher stiffness, the distribution of local strains didn't follow a regular pattern like raw polyurethane foam along the height. The local strains were more distributed and the maximum that it reached was about 86%. Hence, in this case, we didn't experience any case of negative permeability as the combined value of local strain and relative density did not 1. As it is relatively packed, and high local strains were found to be more distributed across the entire cross section of the foam, we can infer that the carbon infused foam is less permeable to intake fire retardants. Irrespective to the foam blocks, the variation of permeability followed the same trend with different values connecting the same curve. This was the same with the case of inertial flow coefficient.

In summary, results of local strain dependent permeability and inertial coefficient from graphs (a) and (b) of figs. 4.6 and 4.7 show that, high local strains lead to low local permeability, low inertial coefficient, high relative density and vice-versa. With in the two foam samples, raw polyurethane foam has higher local permeability and allows a better infusion and dispersion of carbon black. Conversely, the carbon black infused foam is relatively less permeable to fire retardants due to higher local strains .In summary, there is a high likelihood of even distribution of carbon-black liquid onto raw polyurethane foam when compared to the distribution of fire-retardants onto carbon-black foam.

PU	Logarithmic strain	Engineering strain	Permeability, k, (m^2) * 10e-10
	0	0	4.987
	-0.099	-0.094257292	4.070
	-0.335	-0.284661914	2.492
	-0.571	-0.435039804	1.503
	-0.807	-0.553805356	0.884
	-1.043	-0.647604093	0.497
	-1.279	-0.721684523	0.258
	-1.515	-0.780191815	0.114
	-1.751	-0.826399744	0.0362
	-1.987	-0.862893873	0.004
	-2.223	-0.89171623	0.000
	-2.459	-0.914479571	-0.022
	-2.695	-0.932457618	-0.229
	-2.931	-0.946656332	-1.264

Note: Table values represent local strain vs local permeability values

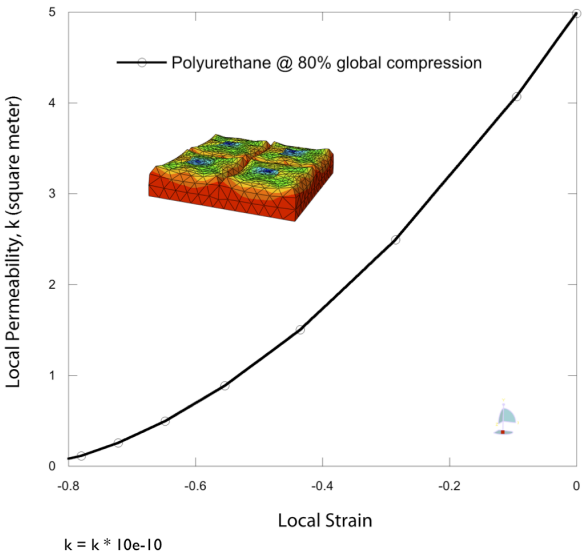

(a) Unidirectional local permeability contour of polyurethane foam

Carbon-black	Logarithmic strain	Engineering strain	Permeability, k, (m^2) * 10e-10
	0	0	4.987
	-0.023	-0.02273752	4.757
	-0.146	-0.1358423	3.695
	-0.315	-0.27021113	2.598
	-0.484	-0.3836868	1.814
	-0.654	-0.48003824	1.253
	-0.823	-0.56088766	0.852
	-0.992	-0.62916572	0.566
	-1.161	-0.68682715	0.363
	-1.330	-0.73552274	0.219
	-1.499	-0.7766466	0.122
	-1.669	-0.81156459	0.057
	-1.838	-0.84086462	0.019
	-2.007	-0.86560876	0.003

Note: Table values represent local strain vs local permeability values

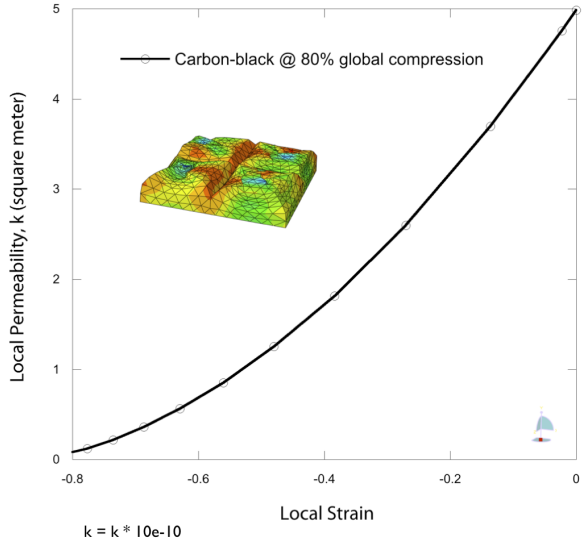

(b) Unidirectional local permeability contour of carbon-black foam

Figure 4.6: Local permeability for polyurethane and carbon-black foams

PU	Logarithmic strain	Engineering strain	Inertial coefficient, B, (m) *10e-10
	0	0	2.233
	-0.099	-0.0942573	2.017
	-0.335	-0.2846619	1.579
	-0.571	-0.4350398	1.226
	-0.807	-0.5538054	0.940
	-1.043	-0.6476041	0.705
	-1.279	-0.7216845	0.508
	-1.515	-0.7801918	0.338
	-1.751	-0.8263997	0.190
	-1.987	-0.8628939	0.063
	-2.223	-0.8917162	0.000
	-2.459	-0.9144796	–
	-2.695	-0.9324576	–
	-2.931	-0.9466563	–

Note: Table values represent local strain vs local inertial coefficient values

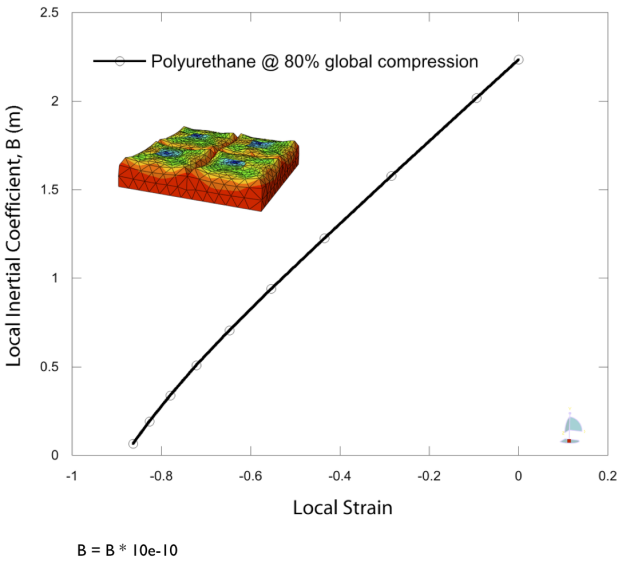

(a) Unidirectional local inertial coeffiicient contour of polyurethane foam

Carbon black	Logarithmic strain	Engineering strain	Inertial coefficient, B, (m) *10e-10
	0	0	2.233
	-0.099	-0.0942573	2.181
	-0.335	-0.2846619	1.922
	-0.571	-0.4350398	1.611
	-0.807	-0.5538054	1.347
	-1.043	-0.6476041	1.119
	-1.279	-0.7216845	0.923
	-1.515	-0.7801918	0.752
	-1.751	-0.8263997	0.602
	-1.987	-0.8628939	0.468
	-2.223	-0.8917162	0.349
	-2.459	-0.9144796	0.238
	-2.695	-0.9324576	0.137
	-2.931	-0.9466563	0.054

Note: Table values represent local strain vs local inertial coefficient values

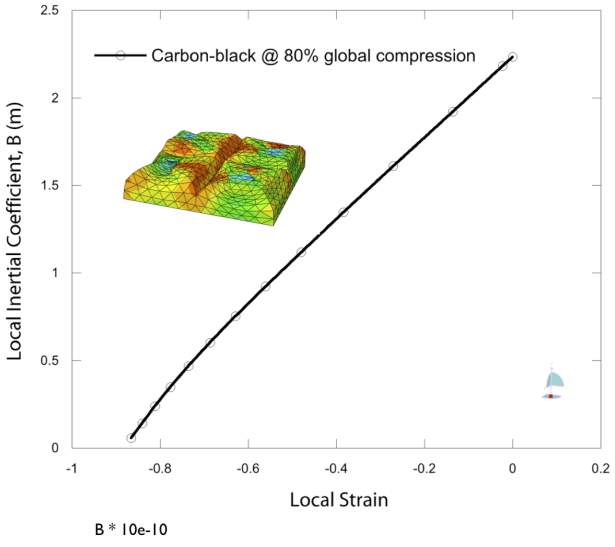

(b) Unidirectional local inertial coefficient contour of carbon-black foam

Figure 4.7: Local inertial coefficients for polyurethane and carbon-black foams

CHAPTER 5

CONCLUSIONS

5.0.1 Vacuum Assisted Infiltration

The initial vacuum assisted infiltration trials for infusion of carbon black in polyurethane foam blocks resulted in higher conductivity of foam samples compared with the current fabrication process. This technique promises to be a potential alternative to the existing fabrication technique followed at ETS-Lindgren and is also environmental friendly. This process also has inherent advantages of less consumption of the fluid as infiltration takes place on a compressed foam block where the open pores are brought closer under compression. As the infiltration occurs in vacuum, it ensures complete impregnation of the fluid and provides homogenous dispersion of the fluid across the foam block.

Vacuum assisted infiltration trials were conducted on six foam blocks and resistance values were measured on all faces of the foam block. The resistance values measured on foam blocks fabricated by vacuum assisted infiltration were almost half that of those values measured on ETS supplied foam. Reduction in resistance values would mean higher the conductivity, a key parameter in the performance of anechoic chambers. Drying time was periodically monitored and these samples were air dried for 30 hours. The samples were not completely dried at this time period. Alternate options of drying were attempted by passing hot air up to 100° from a heat gun into the inlet port for about 20 minutes and the drying rate was monitored. Another attempt was made by passing exhaust air from hot oven at 120° for 30 minutes. Either of them didn't help in drying as the air flow from the heat gun was much faster than the vacuum generated by the vacuum pump and the temperature

rise couldn't be realized inside the vacuum enclosure. Drying time is a parameter which should be worked on improvement and it might be expected by centrifuge drying or by passing these blocks through a hot chamber in in conveyors.

5.0.2 Permeability and Inertial Flow Coefficients

VAI being the primary motivation, the scope of this work was extended to predict the variation of permeability(K) and inertial flow coefficients(B) across the compressed pyramidal foam block used as radio-frequencey absorbers and anechoic chambers. This variation in local permeability can be used for modeling fluid flow using computational fluid dynamics in VAI. The first step in the process of predicting the permeability has been to predict the material parameters of the polyurethane foams. Uniaxial compression were performed on blocks of raw polyurethane foam and blocks infused with carbon black solution. The non-linear stress strain response was used to determine the material parameters that define the nature of elastomeric foams. Shear modulus(μ) and the material constants (α, β) were predicted using a second order Ogden's strain energy function for elastomeric foams. Hence, six material parameters (($\mu_1, \mu_2, \alpha_1, \alpha_2, \beta_1, \beta_2$) were obtained using the curve fitting tool in Matlab®. Care was taken to ensure that the constants derived out of the curve fitting process were realistic with positive values of shear modulus as the same curve could be fit with different material parameters. The material parameters were validated by reproducing the uniaxial compression on solid foam blocks in ABAQUS®. A very close curve fit was obtained between simulations and experiments which validated the accuracy of material parameters.

To predict the permeability of the compressed open cell flexible foams which varies with respect to local strains, a pyramidal block was modeled in Solidworks® and was subjected to uniaxial compression in ABAQUS®. Simulations on the pyramidal block were carried out for material parameters arrived for both raw polyurethane foams and carbon

black infused foams. The meshed model was subjected to uniaxial compression by an analytically rigid plate. Strain contour plots were generated in ABAQUS® for both types of foams. Local strains experienced by raw polyurethane foams were around 90% and above at the sharp tip and nearby proximal zones. Majority of the height of the compressed foam has shown low local strains levels. Low local strains correspond to high local permeability. This would transform into a high likelihood of uniform dispersion of carbon-black liquid into raw polyurethane foam.The permeability decreased with increase in local strain and it was observed that the permeability was negative in the regions which experienced strains of 90% and above. Experiencing a negative permeability is non-pragmatic and this would essentially transform that compressive load applied on a geometry like pyramid should not locally deform the foam block more than 90%, hence making the medium permeable for the flow.

In case of the carbon black infused foam, the local strains were more distributed all across the width of the foam. This could be attributed to the density of the carbon black infused foam which was relatively higher than the raw polyurethane foam, hence making it more stiffer to deformation. The permeability values had a similar trend like raw polyurethane foams but there was no observation of negative permeability unlike raw polyurethane foams. In comparison, carbon black infused foams seemed to be less permeable for infusion of fire retardants.

The inertial flow coefficient governing turbulent flow decreased with increase of local strain values and followed the same trend for both raw polyurethane foams and carbon black infused foam blocks. A practically realistic value was not achieved for local strains more than 90% in case of raw polyurethane foams as they were calculated as the square root of permeability.

Hence, it could be concluded that VAI is a potential alternative to the existing fabrication technique for manufacturing absorber foams. As infusion and permeability are closely related, it could be concluded that complete infusion on the foam block can be achieved under 90% of local strains under compression.

5.1 Scope for Future Work

5.1.1 Simulation of Fluid Flow Across the Compressed Pyramidal Block

The permeability and the inertial flow coefficients can be extended to predict the pressure drop across the foam length [42]. This would be helpful in modeling the fluid flow using CFD considering other parameters like viscosity, density and the velocity of the impregnating fluid. The flow pattern could be visualized for different velocities for different fluids. Also, an extension of the work to monitor the wettabitlity of the fluid on the foam block could prove useful in predicting the optimal location of fluid ports for maximum impregnation of the fluid.

5.1.2 Vacuum Assisted Infiltration Setup for Commercialization

To commercialize the VAI process for large scale infiltration of foams, a VAI mold setup was conceived to ease the process of laboratory setup by eliminating tacky tapes. It consists of a rectangular aluminum plate with a square slot cut in the centre for loading the samples from the bottom side. The cut square slot is covered with rubber seal at it's circumference and this can create a vacuum tight seal when inserted back into the plate. It is also provided with two latches located diametrically opposite to secure it's position with the base plate. Rubber sealing is constructed around the periphery of the base plate on the upper side and adequate vacuum bag to accommodate foam block is spread on the top of the plate. Aluminum bars are rested on the vacuum bag forming a wall around the base plate and can be held in position by a spring clamp. This would ensure intact sealing of the vacuum bag

between the base plate and aluminum bars.The base plate is rested on the supports at all the corners in the bottom side. A representation of the setup is shown in the fig 5.1

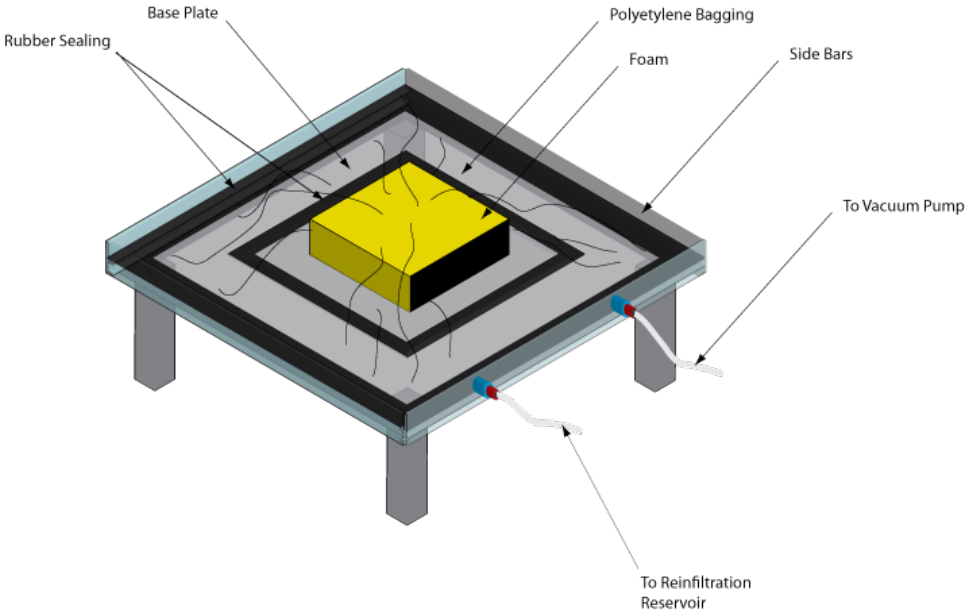

Figure 5.1: A setup for commercializing vacuum assisted infiltration

The loading of the samples takes place from underneath of the base plate by removing the square slot which can be placed back after loading the foam sample. This setup now forms a sealed enclosure similar to the laboratory VAI setup. The aluminum bar on the front view has two openings one of which is connected to the inlet port and the other is connected to the resin trap. These ports pass through the vacuum bagging and sealing has to be ensured by close interference. A vacuum sealed enclosure can be created by activating the motor which pulls vacuum through the resin trap and thereby collapsing the vacuum bag allowing the carbon black to infiltrate.

BIBLIOGRAPHY

[1] Mdiproducts, "Microstructure of closed cell foam,"

[2] ETS-Lindgren, "Anechoic chamber product brochure,"

[3] H. Chinn, U. Lochner, and A. Kishi, "Chemical economics handbook," 2009.

[4] L. J. Gibson and M. F.Ashby, *Cellular Solids : Structure and Properties*. Cambridge University Press, 1997.

[5] ETS-Lindgren, "Rf microwave absorber product brochure,"

[6] R. P. Singh, "Multifunctional composite panels with foam core sandwich,"

[7] A. Erdemir, J. Saucerman, D. Lemmon, B. Loppnow, B. Turso, J. Ulbrecht, and P. Cavanagh, "Local plantar pressure relief in therapeutic footwear: design guidelines from finite element models," *Journal of Biomechanics*, vol. 38, pp. 1798–1806, SEP 2005.

[8] D. Lemmon, T. Shiang, A. Hashmi, J. Ulbrecht, and P. Cavanagh, "The effect of insoles in therapeutic footwear - A finite element approach," *Journal of Biomechanics*, vol. 30, pp. 615–620, JUN 1997.

[9] R. Ragan, T. Kernozek, M. Bidar, and J. Matheson, "Seat-interface pressures on various thicknesses of foam wheelchair cushions: A finite modeling approach," *Archives of Physical Medicine and Rehabilitation*, vol. 83, pp. 872–875, JUN 2002.

[10] W. Chen, C. Ju, and F. Tang, "Effects of total contact insoles on the plantar stress redistribution: a finite element analysis," *Clinical Biomechanics*, vol. 18, pp. S17–S24, JUL 2003.

[11] J. Dionne, M, C. Aubin, J. Dansereau, and R. Aissaou, "Finite element modeling of a wheelchair seat cushion," *11th Conference of the ESB*, vol. , no. , p. , 1998.

[12] N. Mills and A. Gilchrist, "Modelling the indentation of low density polymer foams," *Cellular Polymers*, vol. 19, no. 6, pp. 389–412, 2000.

[13] G. Lyn and N. . J. Mills, "Design of Foam Crash Mats for Head Impact Protection," *The Engineering of Sport*, vol. , no. , pp. 153–163, 2002.

[14] N. J. Mills, *Polymer Foams Handbook*. Elsevier Ltd., 2007.

[15] M. T. Petre, A. Erdemir, and P. R. Cavanagh, "Determination of elastomeric foam parameters for simulations of complex loading," *Computer Methods in Biomechanics and Biomedical Engineering*, vol. 9, no. 4, pp. 231–242, 2006.

[16] Z. Liu and M. Scanlon, "Modelling indentation of bread crumb by finite element analysis," *Biosystems Engineering*, vol. 85, pp. 477–484, AUG 2003.

[17] N. J. Mills and G. Lyn, "Modelling of air flow in impacted polyurethane foam," *Cellular Polymers*, vol. 21, no. 5, pp. 343–367, 2002.

[18] G. Von Der Schulenburg, M. Paterson-Beedle, L. Macaskie, L. Gladden, and M. Johns, "Flow through an evolving porous media compressed foam," *Journal of Material Science*, vol. 42, pp. 6541–6548, 2007.

[19] S. E. Adrian, *The physics of flow through porous media*. University of Toronto Press, 1974.

[20] M. A. Dawson, J. T. Germaine, and L. J. Gibson, "Permeability of open-cell foams under compressive strain," *International Journal of Solids and Structures*, vol. 44, pp. 5133–5145, AUG 1 2007.

[21] S. R. Annapragada, J. Y. Murthy, and S. V. Garimella, "Permeability and thermal transport in compressed open-celled foams," *Numerical Heat Transfer Part B-Fundamentals*, vol. 54, no. 1, pp. 1–22, 2008.

[22] M. Sefton and H. Lusher, "Hydraulic Permeability of Open-Cell Hydrophilic Polyurethane Foams," *Journal of Applied Polymer Science*, vol. 25, no. 10, pp. 2167–2178, 1980.

[23] A. Gent and K. Rusch, "Permeability of Open Cell Foamed Materials," *Journal of Cellular Plastics*, vol. 2, no. , pp. 46–51, 1966.

[24] N. Hilyard and P. Collier, "A structural model of air flow in flexible pur foams," *Cellular polymers*, vol. 6, no. 6, pp. 9–26, 1987.

[25] "Standard test methods for flexible cellular materials - slab, bonded, and moulded urethane foams," *ASTM*, 2001.

[26] P. Muralidharan, "Finite deformation biphasic material characterization and modeling of agarose gel for functional tissue engineering applications," 2006.

[27] R. Ogden, "Large deformation isotropic elasticityon the correlation of theory and experiment for incompressible rubberlike solids," *Proceedings of the Royal Society*, pp. 565–584, 1972.

[28] Simulia, *ABAQUS 6.6 Theory Manual*.

[29] P. B. Thiyagarajan, "Non-linear finite element analysis and optimization for light weight design of an automotive seat backrest," 2008.

[30] R. Ogden, *Non-Linear Elastic Deformations*. Chichester, NY: Ellis Horwood Limited, 1984.

[31] M. T. Petre, "Determining material parameters for multi-axial simulations of elastomeric foams," 2005.

[32] E. Twizell and R. Ogden, "Non-linear optimization of the material constants in ogden's stress-deformation function for incompressible isotropic elastomers," *Journal of the Australian Mathematical Society*, vol. B, no. 24, pp. 424–434, 1986.

[33] J. Zhang, N. Kikuchi, V. Li, A. Yee, and G. Nusholtz, "Constitutive modeling of polymeric foam material subjected to dynamic crash loading," *International Journal of Impact Engineering*, vol. 21, pp. 369–386, MAY 1998.

[34] W. Warren and A. Kraynik, "The Non-Linear Elastic Behaviour of Open-Cell Fams," *Journal of Applied Mechanics-Transactions of the ASME*, vol. 58, pp. 376–381, JUN 1991.

[35] L. E. Malvern, *Introduction to the Mechanics of Continuous Medium*. Englewood Cliffs, NJ: Prentice-Hall, 1969.

[36] Mathworks, *Matlab R2010a user's guide*. 2010.

[37] T. Coleman and Y. Li, "An interior trust region approach for nonlinear minimization subject to bounds," *Siam Journal on Optimization*, vol. 6, pp. 418–445, MAY 1996.

[38] B. Storakers, "On material representation and constitutive branching in finite compressible elasticity," *Journal of the Mechanics and Physics of Solids*, vol. 34, no. 2, pp. 125–145, 1986.

[39] R. Landers, J. Venzmer, and T. Boinowitz, "Methods for cell structure analysis of polyurethane foams,"

[40] R. Herrington, R. Broos, and P. Knaub, "Flexible polyurethane foams - cell size," in *Handbook of Polymeric Foams and Foam Technology* (D. Klempner and V. Sendijarevic, eds.), pp. 97–98, Hanser Gardner Publications, 2004.

[41] M. C. Hawkins, B. O'Toole, and D. Jakovich, "Cell morphology and mechanical properties of rigid polyurethane foam," *Journal of Cellular Plastics*, vol. 41, pp. 267–285, May 2005.

[42] J. G. Fourie and J. P. Du Plessis, "Pressure drop modelling in cellular metallic foams," *Chemical Engineering Science*, vol. 57, pp. 2781–2789, 2002.

VITA

Balaji Ramanujakannan

Candidate for the Degree of

Master of Science

Thesis: PREDICTION OF PERMEABILITY IN COMPRESSED POLYURETHANE FOAMS IN VACUUM ASSISTED INFILTRATION PROCESS

Major Field: Mechanical and Aerospace Engineering (Solid Mechanics & Design)

Biographical:

Personal Data: Born in Pondicherry, Tamilnadu, India, on October, 1983.

Education:

Received the Bachelors degree from Anna University, Chennai, Tamilnadu, India, 2005, in Mechanical Engineering.

Completed the requirements for the degree of Master of Science with a major in Mechanical Engineering Oklahoma State University in May 2011.

Experience:

Worked as a Graduate Research Assistant at the Mechanics of Advanced Materials Laboratory headed by Dr. Raman P. Singh in the area of polymer reinforced composites.

Name: Balaji Ramanujakannan Date of Degree: May, 2011

Institution: Oklahoma State University Location: Stillwater, Oklahoma

Title of Study: PREDICTION OF PERMEABILITY IN COMPRESSED POLYURETHANE FOAMS IN VACUUM ASSISTED INFILTRATION PROCESS

Pages in Study: 53 Candidate for the Degree of Master of Science

Major Field: Mechanical and Aerospace Engineering (Solid Mechanics & Design)

Foams used for radio-frequency(RF) and acoustic shielding were treated with carbon black and cut into pyramidal blocks for better absorption characteristics. The general manufacturing process involves immersion of polyurethane foam blocks in a bath of carbon black solution and fire retardants followed by cutting the blocks into desired pyramidal shapes. The immersion process has inbuilt conductivity variation and impacts the absorption properties apart from resulting in significant quantity of scrap. These scraps needs to be treated chemically before being disposed to landfills which significantly increases overhead costs. A potential alternative to the existing fabrication technique was proposed and hence vacuum assisted infiltration (VAI) was developed successfully for infiltration of carbon black mixture into foams.

With VAI on foams being the preliminary motivation, this work predicts the variation of local permeability along the cross-section of the foam under compression. These permeability values can be used to model the fluid flow using computational fluid dynamics to determine the location of the inlet and outlet ports in VAI process to achieve homogenous infiltration. An extended version of the Darcy's flow equation for porous media forms the basis of the governing equation. As the infiltration happens in a compressed block of foam, Permeability(K) varies with compression and is dependent on strain. Uniaxial compression experiments were carried out to obtain the stress-strain curves on a cubical foam block and this curve was fit to Ogden's material model for elastomeric foams in Matlab® to obtain material parameters. This experiment was duplicated in ABAQUS® to validate the predicted material parameters. These material parameters were then used to simulate uniaxial compression of pyramidal blocks in ABAQUS® for determining local strains. Variation in local permeability was determined from local strains across the height of the compressed block using the equations developed by Hilyard and Collier.

ADVISOR'S APPROVAL: Dr.Raman P.Singh